

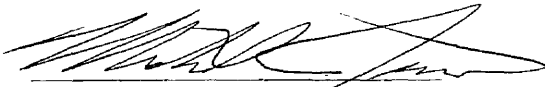
# Developmental Changes in Gene Expression in the Visual Cortex of Mice with Retinal Degeneration

by

Ashley M. Cornett

Thesis submitted to the Faculty of the  
University of Michigan – Flint  
in partial fulfillment of the  
requirements for the degree of  
Master of Science in Biology

Approved By:



Dr. Michael Jarvinen  
Thesis Advisor  
Dept. of Psychology



Dr. Joseph Sucic  
Thesis Advisor  
Dept. of Biology



Dr. Ann Sturtevant  
Reader  
Dept. of Biology

University of Michigan-Flint  
May 2008

# Developmental Changes in Gene Expression in the Visual Cortex of Mice with Retinal Degeneration

by  
Ashley M. Cornett

Joseph F. Sucic,  
Chairman Biology

## Abstract

Retinal degeneration can be caused by many genetic mutations. The Pde6b-mutation affects rod photoreceptors, which are lost in mice by post-natal day (PND) 21 (Marc et al., 2003; Chang et al., 2002). Mice that are homozygous for the Pde6b-mutation are born with vision and go blind over time. Behavioral studies suggest that Pde6b- mice lose their visual acuity by age PND 42 and subsequently lose their ability to detect differences in light illumination by PND 100. Behavioral changes have been correlated with changes in gene expression in specific cells in earlier studies. In this study, gene expression changes were examined for astrocytes in the visual cortex using real-time PCR for astrocyte-specific genes GFAP, Vimentin and S100. GFAP and vimentin have been found to be useful for identifying the link between behavioral changes and their corresponding gene expression pattern changes (Kafitz et al., 1999). S100 mRNA expression is also useful because it can influence GFAP and vimentin at the protein level (Muller et al., 1993). It was hypothesized that astrocyte-specific gene expression changes will be found at relevant ages (PND 21, 42 and 100) in astrocytes of the visual cortex in our Pde6b- mice compared to Pde6b+ mice, due to remodeling after a loss of visual function indicated by behavioral changes at these ages. We hypothesize that GFAP expression will decrease, vimentin expression will increase and we are not

sure what will happen to the expression of S100 at these relevant ages. Results suggest that changes in gene expression are taking place at PND 7, 21 and 49. Our hypothesis may not be fully supported at the ages where behaviors were changing, but our data do suggest changes in gene expression at other possibly relevant ages. PND 21 was the age that showed a change in gene expression for vimentin coinciding with the age that rod photoreceptors are lost. This age could be examined further at the protein level for the glial genes.

## Acknowledgements

First I would like to thank my husband, Michael Cornett, who has encouraged me through graduate school every step of the way. I would not have been able to accomplish this without him. As a newly-wed couple that does not live under the same roof, no one would disagree that Michael is a very patient and understanding individual. Michael makes me strive for my best. Next, I would like to thank my family for supporting me the entire time I have pursued my education. I could not have gotten this far without them. I would also like to thank my friend and fellow graduate student, Ghada Sharif, not only for her listening skills but also for her encouraging words. We started together and have been on the same boat for the majority of our classes and research, which made the biology department hall much more fun! I would also like to thank her and Nickole Hatley for their expertise in cloning and transforming. I thank Dr. Sucic for letting me work in his laboratory and for letting me ask countless, hopefully intelligent, questions. I really enjoyed working in this laboratory, not only because of Dr. Sucic, but also because of the many students involved in molecular biology research. I thank Natalie Walker, Matthew Eckwahl and Arasakumar Subramani for asking questions and discussing my research with me. Next, I would like to thank Dr. Jarvinen because his is the project I have been working on for the past year and also for helping me guide this research project in the right direction and letting me take the lead. Thank you Dr. Sturtevant for the initial help with real-time PCR: it would have been a lot harder to get that part of the project off the ground without it. I want to thank Krishnapriya Chinnaswamy for assisting me with many aspects of the project. Priya came into the project eager and

motivated and really picked up the pace by taking over the RNA extraction, DNase treatment, and cDNA synthesis (plus the RT-control PCR). Thank you so much! Thank you to Dennis Viele for discussing statistics with me during the analysis. Also, I would like to thank some very helpful ladies from Eppendorf: Renee Davis and Beverly Wohl, who have answered more than one question I had about my real-time PCR results. I would like to thank Larry Atherton for helping me order supplies and helping to make sure everything was set up in the new lab for me. I would like to thank Dr. D.J. Trela, Dean of the College of Arts and Sciences at the University of Michigan-Flint, for funding part of my thesis project. Lastly, I would like to thank both University of Michigan-Flint College of Arts and Sciences and Office of Research for helping with statistics.

## Table of Contents

Abstract.....	ii
Acknowledgements.....	iv
List of Figures.....	viii
List of Tables.....	ix
List of Graphs.....	x

### Chapter One: History & Introduction

1) Links between behavior and specific brain areas/cell types: brain remodeling and plasticity.....	1
2) Vision loss (Pde6b <sup>-</sup> mice) and behavior change.....	2
3) Astrocytes and their involvement in plasticity: GFAP, vimentin and S100.....	9
4) Gene expression analysis: end-point and real-time PCR.....	14

### Materials and Methods

1) Brain tissue samples: Pde6b <sup>-</sup> and Pde6b <sup>+</sup> mice.....	15
2) RNA extraction.....	15
3) cDNA synthesis.....	15
4) End-point PCR using GAPDH and gel electrophoresis.....	16
5) Quantitative real-time PCR.....	16
a. Real-time PCR primers.....	16
b. Cloning of real-time PCR products into pCR <sup>®</sup> 4-TOPO.....	17
c. Transformation into XL1-Blue.....	17
d. Overnight cultures of transformed bacteria.....	17
e. Plasmid preps, analysis and sequencing.....	18
f. Real-time PCR using QuantiFast SYBR Green.....	18
i. Background and color (SYBR Green) calibration.....	18
ii. Real-time PCR optimization of GAPDH and astrocyte-specific genes.....	18
1. cDNA amount and final concentration optimization.....	18
2. Temperature optimization.....	22
3. Primer concentration optimization.....	23
g. Standard and efficiency curves.....	24
h. Real-time PCR procedure for individual runs.....	26
i. Data analysis criteria.....	29

### Chapter Three: Results

1) Standard and efficiency curves analysis.....	31
2) Raw data analysis using correlation.....	31

3) $\Delta$ Ct data analysis using parametric and non-parametric tests.....	32
---	----

## **Chapter Four: Discussion**

1) Raw data analysis.....	38
2) Standard and efficiency curves analysis.....	41

## **Literature Cited**

## **Appendices**

1) Data for standard and efficiency curves analysis.....	46
2) Regression analysis output for standard and efficiency curves.....	47
3) Syntax for regression analysis using SPSS.....	51
4) Data: high and low Ct values for each sample.....	52
5) Correlation analysis syntax using SPSS.....	53
6) GFAP SPSS correlation statistics.....	54
7) Vimentin SPSS correlation statistics.....	56
8) S100 SPSS correlation statistics.....	59
9) GAPDH SPSS correlation statistics.....	62
10) Data: $\Delta$ Ct values.....	65
11) $\Delta$ Ct t-test analysis syntax using SPSS.....	66
12) T-test output each gene/age using SPSS.....	66
13) Graphing $\Delta$ Ct for each gene syntax using SPSS.....	73
14) Syntax for non parametric test kruskal-wallis Test.....	73
15) Non-parametric kruskal-wallis test output each gene/age using SPSS.....	73

## List of Figures

Figure 1:	Phosphodiesterase type 6.....	3
Figure 2:	Phase 1 of light illumination behavior test.....	7
Figure 3:	Phase 2 of light illumination behavior test.....	7
Figure 4:	Phase 3 of light illumination behavior test.....	8
Figure 5:	Sensory perception pathways.....	9
Figure 6:	Amplification plot for real-time PCR.....	21
Figure 7:	Melting curve for real-time PCR.....	22
Figure 8:	Real-time PCR reaction set up in a 96-well plate for individual runs.....	28
Figure 9:	Pde6b- (RD) mouse behavior and gene expression time-line.....	38



## List of Tables

Table 1:	Details of PCR products and successful primers used for each gene in our study.....	17
Table 2:	Reaction component variations used during optimization of real-time PCR primers.....	19
Table 3:	Gradient of annealing temperature optimization used for GAPDH and astrocyte-specific genes.....	23
Table 4:	Matrix of final upstream versus downstream primer concentration.....	24
Table 5:	Reaction components used during primer concentration optimization.....	24
Table 6:	Parameters of each optimized gene.....	24
Table 7:	Gradient of annealing temperatures used for data collection runs.....	27
Table 8:	Regression analysis and confidence interval values.....	32
Table 9:	Correlation summary: r values and significance levels for each unique gene/age.....	34

## List of Graphs

Graph 1: Summary of data from each phase of the light illumination behavior test.....	8
Graph 2: Scatter plot of standard and efficiency curves with regression line.....	33
Graph 3: Mean GFAP $\Delta$ Ct for wild type and retinal degeneration over time.....	35
Graph 4: Mean S100 $\Delta$ Ct for wild type and retinal degeneration over time.....	36
Graph 5: Mean vimentin $\Delta$ Ct for wild type and retinal degeneration over time.....	37

## **Chapter One: History & Introduction**

### **Links between behavior and specific brain areas/cell types: brain remodeling and plasticity**

Behavioral changes are tied to changes in specific brain areas as well as specific cell types. The ability of the brain to change is called brain plasticity. This is not a new idea; many studies have demonstrated this in the past (Kafitz et al., 1999). One example is seen in canaries. Every spring, mature male canaries learn an elaborate song in order to find a mate. The brain region responsible for male canaries learning a song is the higher vocal center (HVC), that when damaged will result in the loss of the song behavior (Kafitz et al., 1999). Interestingly, songbirds can sing only during the springtime. This is when significant morphological changes are occurring in HVC neurons (Kafitz et al., 1999). The morphological changes found in HVC neurons are mirrored in HVC astrocytes at the same time (Kafitz et al., 1999). Astrocytes can guide neurons by regulating neurite extension and outgrowth and neural synapse formation during remodeling (i.e. plasticity) (Kafitz et al., 1999; Rochefort et al., 2002; Privat, 2003; Argandona et al., 2003). Kafitz et al. (1999) demonstrated seasonal changes in patterns of gene expression in astrocytes in the HVC of male canary brains.

Vimentin and Glial Fibrillary Acidic Protein (GFAP) were used as astrocyte-specific cell markers (Kafitz et al., 1999). Vimentin and GFAP are type III intermediate filament proteins (Matsuzawa et al., 1997) that can be visualized via labeling with their respective antisera. Immature astrocytes are labeled with vimentin antisera and mature astrocytes are labeled using GFAP antisera (Kafitz et al., 1999). Kafitz et al. found that

vimentin expression increased while the songs were becoming stable and concluded that vimentin promotes brain plasticity. They also found that GFAP expression increases when the song was stable and concluded that GFAP inhibits brain plasticity. These results suggest that behavioral changes may be triggered by gene expression changes in specific cell types. This model of brain plasticity can be applied to other situations where behavioral changes are linked to modifications in gene expression. Our study focused on changes in gene expression corresponding to behavioral changes due to retinal degeneration. The behavioral studies, discussed later, identify potentially important time points to examine gene expression pattern changes in the visual cortex. It is hypothesized that we will find gene expression pattern changes in specific cell types at relevant time points during development.

### **Vision loss (Pde6b- mice) and behavior change**

Vision loss can be caused by many different genetic mutations. Retinal degeneration (RD) can cause photoreceptor death, which ultimately results in vision loss (Chang et al., 2002). Mouse models have been used to investigate retinal degeneration to elucidate the mechanism of photoreceptor death (Chang et al., 2002). Chang et al. summarized 16 different mouse models of retinal degeneration affecting mice at varying ages and genome locations. Two of these RD mice have mutations in the gene encoding the beta subunit of phosphodiesterase type 6 (Pde6b), located on mouse chromosome 5 (Pde6b<sup>rd1</sup> and Pde6b<sup>rd10</sup>) (Chang et al., 2002). Phosphodiesterase Type 6 (Pde6) contains three subunits: alpha, beta and gamma (Figure 1). Wild type Pde6b codes for the beta

subunit. The main function of Pde6 beta and alpha is to hydrolyze cGMP when active and be inhibited by Pde6 gamma when inactive (Ionita et al., 2007).

**Figure 1: Phosphodiesterase type 6**

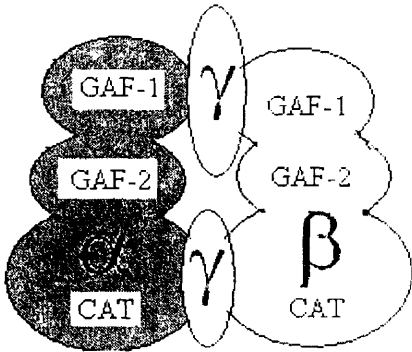


Figure 1: Proposed structure of phosphodiesterase type 6, showing its three subunits and the domains of the alpha ( $\alpha$ ) and beta ( $\beta$ ) subunits. GAF-1 and GAF-2 are non-catalytic cGMP binding domains, and CAT is the catalytic domain. Pdb6 gamma ( $\gamma$ ) is in this model to illustrate the two binding domains on each of the  $\alpha$  and  $\beta$  subunits. (This figure is derived from the model in Ionita et al., 2007).

Pde6 is found in rod photoreceptors and is of significant importance in the phototransduction cascade (Ionita et al., 2007). This enzyme regulates the levels of rod excitation in the presence and absence of light stimulation (Ionita et al., 2007). During light stimulation rhodopsin is activated, which in turn activates transducin, a G-protein, by causing it to exchange GDP for GTP. GTP-transducin activates Pde6 by displacing its gamma subunits (Blumer, 2004; Ionita et al., 2007). When activated, the Pde6 alpha and beta catalytic sites hydrolyze cGMP to GMP, decreasing the intracellular level of cGMP. Decreased levels of cGMP close the cGMP-gated  $\text{Na}^+$  ion channels and cause hyperpolarization of the rod plasma membrane (Blumer, 2004; Ionita et al., 2007). This activates rod photoreceptors and causes a signal to be sent to the brain. In the absence of light other enzymes in the phototransduction pathway turn off the light-induced response

by increasing the rate at which transducin hydrolyzes its bound GTP (Blumer, 2004; Ionita et al., 2007). This yields the inactive GDP-transducin leading to cGMP-gated ion channels opening and polarization returning to normal (Blumer, 2004; Ionita et al., 2007).

Pde6b<sup>rd1</sup> mice have a murine viral insert plus a nonsense mutation in the 7<sup>th</sup> exon of the Pde6b gene (Chang et al., 2002). This causes production of a truncated and non-functional form of Pde6b protein (Jones and Marc, 2005). The non-functional Pde6b protein ultimately leads to rod photoreceptor degeneration, which is followed by cone degeneration due to a mechanism illustrated by Marc et al. (2003). Mice homozygous for this mutation experience severe retinal degeneration (Chang et al., 2002).

Pde6b<sup>rd1</sup> strain FVB/N-Tg(GFAPGFP)14Mes/J (stock #003257) from Jackson Laboratories (JAX<sup>®</sup> Mice and Services; Bar Harbor, MA) was chosen for the retinal degeneration strain of mice. Henceforth, this strain will be called Pde6b- or retinal degeneration (RD) mice. These transgenic mice are useful because they have the gene encoding a mutant form of green fluorescent protein (GFP; mutant hGFP-S65T) inserted into their genome under the control of the astrocyte-specific promoter for GFAP (JAX<sup>®</sup> Mice and Services; Bar Harbor, MA). The GFP gene, derived from a jelly fish, *Aequorea victoria*, will emit fluorescence when subjected to a 488nm light source and illuminate the astrocytes expressing ample GFP (used as an indirect measure of GFAP expression) (JAX<sup>®</sup> Mice and Services; Bar Harbor, MA).

Pde6b<sup>rd1</sup> strain FVB.129P2-Pde6b+ Tyr<sup>c-h</sup>/AntJ (stock #004828) from Jackson Laboratories (JAX<sup>®</sup> Mice and Services; Bar Harbor, MA) was chosen for the wild type, control strain. These mice will be called Pde6b+ or wild type (WT). These mice do not

suffer from retinal degeneration because they are homozygous for the wild type Pde6b allele (JAX<sup>®</sup> Mice and Services: Bar Harbor, MA).

The Pde6b<sup>-</sup> mice have phenotypically normal vision at birth and with time lose their vision completely. First, Pde6b<sup>-</sup> mice lose night vision via death of rod photoreceptors. Next, their cones begin to degrade leading to a loss of visual acuity. Visual acuity can be defined as the sharpness or focus in vision. Cone function degrades until there are too few cones present to function properly, leading to a loss of the ability to detect differences in light illumination (having this ability is similar to being able to see that individual ceiling tiles are lit up rather than the entire ceiling being illuminated). Elegant behavior tests were done to establish the time point of each stage of vision degradation. Dr. Jarvinen and undergraduate students in the Psychology Department of the University of Michigan-Flint did these tests, summarized below.

To determine when visual acuity was lost, the Pde6b<sup>-</sup> mice were lowered down over sand paper of different grades (smooth, medium and coarse). The mice were held by the tail and quickly lowered down to the surface of each grade of sand paper where they would splay their legs (or not) before impact. If the mice had normal vision, they would splay their legs before impact on all sand paper grades. Retinal degeneration became apparent when the mice would lose their ability to react to the smooth, and later medium, sand paper and would not splay their legs. When the mice would no longer splay their legs for the coarse sand paper, visual acuity was lost. Behavior changed and visual acuity was lost in RD mice by post-natal day (PND) 42.

To determine when the ability to discriminate between differences in light illumination was lost, the Pde6b<sup>-</sup> mice were subjected to a series of experimental settings

called phases. The phases were set up in a box with gridlines in a controlled room where no distractions would influence the mouse's behavior. The mice were measured for time spent in each square of the grid. Phase 1 was set up so that the light shining down into the box was most intense in one particular corner (Figure 2). Here the mice spent equal amounts of time in each square on the grid (Graph 1). Phase 2 was set up in the absence of light with an interesting smell (pheromone) placed in a corner (i.e., where the light was most intense from Phase 1) (Figure 3). The bedding was changed with each new phase as a control measure. Here the mouse spent significantly more time in the "scent square," or "Hot" partition (Graph 1). The mouse associated the interesting smell with the partition from the amount of light that was previously in that partition from phase 1. Phase 3 was set up the same as phase 1 (Figure 4): mice spent significantly more time in the square where the scent used to be, the "Hot" partition until they were incapable of detecting differences in light illumination (Graph 1). It was found that Pde6b- mice are capable of detecting differences in light illumination until PND ~100, or between PND 91 and 112 (Graph 1).

Data from other laboratories suggest that Pde6b- mice lose rods by PND 21 (Marc et al., 2003; Chang et al., 2002). Rods are located in the outer nuclear layer (ONL) of the retina (Marc et al., 2003) and the ONL is lost in mice homozygous for the Pde6b- allele by PND 21 (Chang et al., 2002); therefore, rods were lost by PND 21. The behavioral tests described above suggest that these mice lose visual acuity by PND 42 and lose the ability to detect differences in light illumination by PND 100. These behavior experiments set the stage for molecular studies by giving specific time points to monitor for potential changes in gene expression. The important time points PND 21 (loss of



night vision), 42 (loss of visual acuity) and 100 (loss of the ability to detect differences in light illumination) are when we expect to find changes in gene expression.

**Figure 2: Phase 1 of light illumination behavior test**

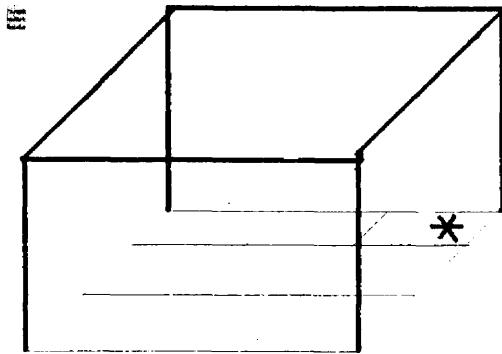


Figure 2: Phase 1 of behavioral test to see if the mice can discriminate between differences in light illumination. This phase had light only: the Pde6b- mice spent equal amounts of time in each square. Square with most intense light is indicated by an asterisk (\*).

**Figure 3: Phase 2 of light illumination behavior test**

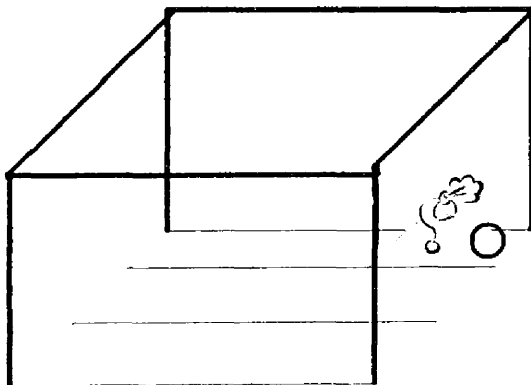


Figure 3: Phase 2 of behavioral test to see if the mice could discriminate between differences in light illumination. This phase has an interesting scent only: the mice spent significantly more time in smell square, which had the most light. The square with the interesting smell was considered the “Hot” partition indicated here with a circle (O). The Pde6b- mice learned to associate the intense light with the interesting smell.

**Figure 4: Phase 3 of light illumination behavior test**

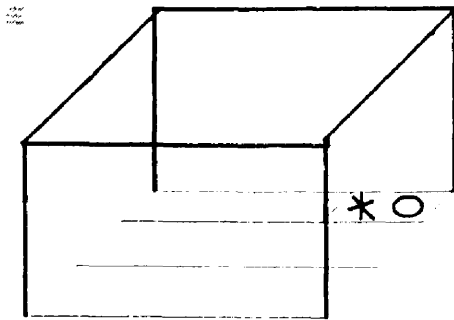
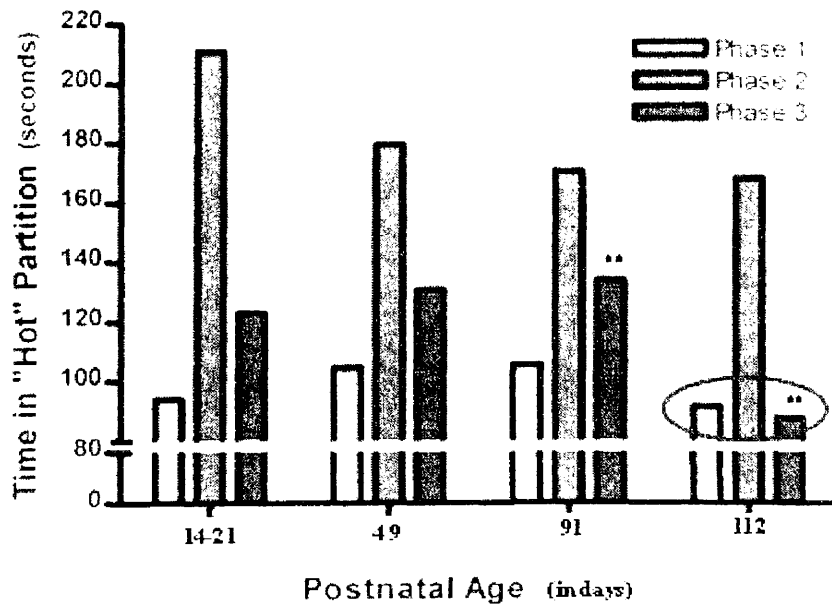


Figure 4: Phase 3 of behavioral test to see if the Pde6b- mice can discriminate between differences in light illumination. This phase was set up with light only: the mouse spent significantly more time in the square where the scent was (indicated by O) until the ability to detect differences in light illumination was lost (the well lit square indicated by \*).

**Graph 1: Summary of data from each phase of the light illumination behavior test**



Graph 1: Summary of data from behavioral test determining at what age Pde6b- mice lost their ability to detect differences in light illumination (Phase 1: light only; Phase 2: scent only; Phase 3: light where scent was). The square with the interesting smell was considered the "Hot" spot or partition. \*\*Significant difference in time spent in "Hot" Partition of phase 3 was seen between PND 91-112.

For the molecular studies, we studied changes in gene expression in the visual cortex. The rationale behind choosing the visual cortex was two fold. First, the eye sends information directly to the thalamus and then to the visual cortex (Figure 5). One could argue that the better place to sample would have been the thalamus. However, the thalamus was not sampled because that region of the brain is difficult to excise in its entirety. In contrast, Dr. Jarvinen was confident that each time he removed the visual cortex, he had isolated all of it and the sample contained no other tissue.

**Figure 5: Sensory perception pathways**

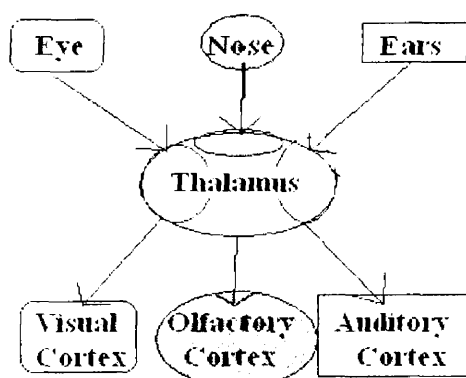


Figure 5: During sensory endocrine, information is passed through the thalamus before further processing in the sensory cortices.

### **Astrocytes and their involvement in plasticity: GFAP, vimentin and S100**

As previously shown by Kafitz et al. (1999), astrocyte cells are critically important for neural plasticity. Astrocytes are a class of glial cells that have been found to play an active roll in synaptogenesis of neural cells in the brain (Ullian et al., 2004). Astrocytes compose almost 50% of the cells in the brain (Ullian et al., 2004) and are found to compose about 28% of the cells in the visual cortex (Gabbott and Stewart.,

1987). They can be recognized by their morphology: these cells have many processes (Argandona et al., 2003), which reach out and form complex networks with surrounding neurons and interneuron synapses (Piet et al., 2003). In the past, astrocytes were thought to be passive cells that nourished neurons and provided them with a favorable environment (Rocheffort et al., 2002, Ullian et al., 2004). Astrocytes do provide neurons with an energy supply and an ion balance, but they are also involved in plasticity where they guide neural axons and regulate neural activity (Rocheffort et al., 2002; Privat, 2003; Argandona et al., 2003).

When stimulated, neurons release neurotransmitters from their axons into the synapse in order to communicate with other neurons (Piet et al., 2003). It has been found that these neurotransmitters are not always kept confined to the synapse where they were released, but can travel into the extracellular space and stimulate neighboring neurons (Piet, et al., 2003). This is called intersynaptic crosstalk (Piet et al., 2003). Astrocytes have been found to be key regulators of intersynaptic crosstalk *in vitro*: independent synapses show increased crosstalk when astrocyte processes were withdrawn suggesting the ability of astrocytes to regulate the activities of neurons (Piet et al., 2003).

It has also been found that the majority of the brain's synaptic structure is formed by PND 21 in mice (Ullian et al., 2004). The astrocyte-specific cell marker found in immature astrocytes is an intermediate filament (IF) protein called vimentin (Dahl et al., 1981; Privat, 2003; Kafitz et al., 1999; Messing and Brenner, 2003). After PND 21, mature astrocytes can be identified with another IF protein called GFAP (Privat, 2003; Kafitz et al., 1999; Messing and Brenner, 2003) along with S100, a calcium binding

protein (Argandona et al., 2003; Muller et al., 1993). GFAP, vimentin and S100 are believed to be important for regulating the interactions between astrocytes and neurons.

GFAP and vimentin are IF type III proteins that help maintain astrocyte cell structure and integrity (Argandona et al., 2003; Goldman et al., 1996). GFAP was first isolated in brain plaques of multiple sclerosis patients over 35 years ago by Larry Eng (Eng et al., 2000). The function of GFAP in astrocytes was elucidated in a murine model using both null (no protein) and modified (elevate protein) alleles of the GFAP gene (Messing and Brenner, 2003). They found only subtle effects without GFAP expression during development (GFAP null mice). This could be explained by the presence of vimentin earlier in development. Interestingly, they found significant phenotypic effects in mice having elevated expression of GFAP (GFAP elevated mice), with similar symptoms to Alexander's disease, a serious neurodegenerative disorder. Symptoms include developmental delays and changes in physical characteristics. One explanation of this disorder caused by the elevated expression of GFAP could be due to a toxic intermediate in the assembly of this IF protein (Messing and Brenner, 2003).

Another study also found that excess GFAP is detrimental to the nervous system's ability to be plastic. Privat (2003) found that expression of GFAP in mice that experience CNS injuries results in a lower rate of neuronal survival and neurite extension. This is most likely due to mature GFAP-expressing astrocytes stabilizing previously made neural connections and impeding the process of establishing new ones. Privat also found that mice expressing vimentin alone had a better ability to form new neural connections post-CNS injury. This again suggests that immature, vimentin-expressing astrocytes promote neural plasticity.

As discussed earlier, Kafitz et al. (1999) also found that immature, vimentin-expressing astrocytes promote plasticity while mature, GFAP-expressing astrocytes inhibit plasticity. The expression of these two glial genes is of interest to our study in relation to Pde6b- mice development. Theoretically, these mice need to have the ability to make changes in their brains due to the loss of a very crucial sense (vision). Once remodeling takes place (i.e. auditory senses enhanced), these changes must then become stable (i.e. inhibition of plasticity). For remodeling to occur, we would expect to see an increase in the expression of vimentin. For subsequent stability to secure these newly remodeled neural pathways, we would expect to see an increase in GFAP expression.

The last protein of interest in this study is S100, a calcium binding protein that was first isolated from a cow's brain in 1965 by Moore (Muller et al., 1993). The S100 protein family has 21 members (Donato, 2003), of which the S100B form is most common in astrocytes in the brains of mammals (Rothermundt et al., 2003). S100 proteins exist functionally as homodimers that become activated by calcium (Donato, 2003). This promotes a conformational change that allows S100B to bind to target proteins such as GFAP and vimentin (Donato, R., 2003). The functional consequence of this interaction is not completely understood.

S100 proteins have been seen to have regulatory activities both intracellularly and extracellularly. Intracellularly, S100B regulates protein phosphorylation, the dynamics of cytoskeleton constituents, calcium homeostasis, etc. (Danato, 2003). In particular, S100B inhibits the phosphorylation of GFAP and vimentin (Rothermundt et al., 2003). It is suggested that binding of calcium-activated S100B to GFAP and vimentin prevents the assembly of the intermediate filament proteins by holding individual subunits and

sequestering them (Donato, 2003; Rothermundt et al., 2003). S100 proteins are mainly located in the astrocyte cell body rather than the processes (Argandona et al., 2003). It has been found that S100 proteins are expressed at the same time points as GFAP in mature astrocytes, with the greatest concentration seen during senescence (Muller et al., 1993). Extracellularly, S100 has been found to regulate the activities of neurons and other astrocytes (Donato, 2003). The extracellular concentration of S100 is crucial for physiological effects. In nanomolar concentrations, S100 has been found to regulate astrocytes and neural activity normally; S100B stimulates neurite outgrowth and enhances the survival of neurons and astrocytes (Rothermundt et al., 2003). In micromolar concentrations, S100 becomes toxic to the surrounding tissue. S100B stimulates the expression of  $\beta$ -amyloid protein which in turn stimulates the expression of S100B: this induces apoptosis in several types of neural cells (Rothermundt et al., 2003).

Clearly, GFAP, vimentin and S100 are of enormous interest when studying the plasticity of the visual cortex in mammals. The present study examined the expression of genes encoding these proteins in the visual cortex of our murine model at specific time points throughout development. It was hypothesized that astrocyte-specific gene expression changes at PND 21, 42 and 100 in astrocytes of the visual cortex in our Pde6b<sup>-</sup> mice compared to Pde6b<sup>+</sup> mice. We hypothesize that GFAP expression will decrease, vimentin expression will increase and we are not sure what will happen to the expression of S100 at these ages. We initially chose to examine the gene expression changes in our murine model first by using end-point PCR. This subsequently led us to a more effective method of relative quantification of gene expression, real-time PCR.

## **Gene expression analysis: end-point and real-time PCR**

End-point PCR is a well-known tool to amplify a gene (genomic DNA) or a copy of an expressed gene (cDNA made from mRNA) (Valasek and Repa, 2005). This was the first technique employed in our project to determine relative gene expression of our genes of interest (GFAP, vimentin and S100). GAPDH, a reference gene encoding glyceraldehyde 3-phosphate dehydrogenase, was also examined. GAPDH is expressed ubiquitously and constitutively in cells, and its expression should not change in a particular cell even when under experimental treatments (Sambrook and Russell, 2001). End-point PCR techniques were time consuming, arbitrary and possibly bias and could not detect the very low levels of expression that we wanted to examine. Real-time PCR was used as a more reproducible, quantitative alternative. I was able to select a kit suitable for the project: QuantiFast™ SYBR® Green PCR Kit (QIAGEN: Valencia, CA) and learn how to use the Mastercycler ep *Realplex*<sup>4</sup> from the manual (Eppendorf: Westbury, NY). Real-time PCR can detect as few as 5 copies of an mRNA transcript (Valasek and Repa, 2005), and the time between setting up a reaction and analysis was typically one fifth that of end point PCR and results proved to be much more reliable. The relative quantification method was used for our real-time PCR study (discussed in detail later).



## **Chapter Two: Materials and Methods**

### **Brain tissue samples: Pde6b- and Pde6b + mice**

Dr. Jarvinen euthanized, decapitated, and removed mouse brains into an ice-cold buffer solution. In total, 64 mice were used in this study (32 Pde6b- and 32 Pde6b+), with 10 ages sampled (PND 7, 14, 21, 28, 35, 42, 49, 100, 140 and 250). Each unique genotype/age had a sample size of three mice with the exception of PND 100 that had a sample size of 5 mice for each genotype. Dr. Jarvinen excised the visual cortex, keeping the mass of each tissue sample equal between animals.

### **RNA Extraction**

RNA was extracted from each brain tissue sample using the PureLink™ Micro-to-Midi Total RNA Purification System as instructed by the manufacture (Invitrogen: Carlsbad, CA). The RNA sample was stored at -70°C, or used in DNase treatment. DNase I, Amplification Grade, was purchased from Invitrogen and used as instructed by manufacturer. DNased RNA samples were also stored at -70°C until used in cDNA synthesis.

### **cDNA synthesis**

cDNA synthesis was carried out as instructed by the manufacture using SuperScript™ III First-Strand Synthesis System for RT-PCR (Invitrogen). cDNA synthesis procedures were repeated for every DNase treated RNA sample plus a reverse transcription control. The reverse transcription control was exactly the same as the

cDNA synthesis but added additional water to make up for the absence of reverse transcriptase, which was called Pseudo-cDNA. This was a control that tested for contamination of the reagents in cDNA synthesis.

### **End point PCR using GAPDH and gel electrophoresis**

Both real cDNA and pseudo-cDNA were used to make GAPDH PCR products. This tested the pseudo-cDNA for contamination while confirming the real cDNA was intact. These PCR products were subjected to 1% agarose gel electrophoresis in 0.5x TBE Buffer for 1 hour at 90 volts. The gel was stained with Ethidium bromide (EB) and de-stained in tap water. If the cDNA reagents were contaminated we would see PCR product in the pseudo-cDNA samples. Each of our sample cDNAs were tested for a single product of 561 bps and to verify there was no contamination. Amplification of pseudo-cDNA did not produce any bands.

### **Quantitative real-time PCR**

#### **Real-time PCR primers**

Each primer set was designed using Laser Gene Software (DNASTAR; Madison, WI). Sequences of mouse GAPDH, GFAP, Vimentin and S100 genes were obtained from GenBank ([www.ncbi.nlm.nih.gov/Genbank](http://www.ncbi.nlm.nih.gov/Genbank); accession numbers XR\_031086.1 [GAPDH], NM\_010277.2 [GFAP], NM\_008691.2 [Vimentin], NT\_039510.2 [S100]). The range of product size for real-time PCR is between 100-200 bps and the primers were designed accordingly (Table 1).

## Cloning of real-time PCR products into pCR<sup>®</sup> 4-TOPO

Each primer set was used to make a PCR product that was used in cloning. PCR products were ligated into pCR-4 TOPO cloning vector by Nickole Hatley and Ghada Sharif using the TOPO TA Cloning<sup>®</sup> Kit for Sequencing (Invitrogen), as directed by manufacturer's instructions.

**Table 1: Details of PCR products and successful primers used for each gene in our study**

Gene	Sequence of real-time Primers (Up and Down)	Size of PCR Product (base pairs)
<b>GFAP</b>	5'-TTGCAGACCTCACAGACGCTGCGT-3' (781-802) 5'-GCATGGCGCTCTTCCTGTT-3' (940-958)	<b>172</b>
<b>S100</b>	5'-TAAGAATCAAGGCAGACTACCAA-3' (731-753) 5'-GTCTGTCTACTTCTGGAGCAT-3' (882-903)	<b>173</b>
<b>Vimentin</b>	5'-GCCAAATCCCCTATGCCCAAATCA-3' (1838-1861) 5'-CCTTCTTTTATCTGCAACATCTT-3' (2007-2030)	<b>193</b>
<b>GAPDH</b>	5'-GGCAAGGTCATCCCAGAGC-3' (704-722) 5'-CCTTCAGTGGGCCCTCAGATGC-3' (845-866)	<b>163</b>

Table 1: Sequences of upstream and downstream primers for real-time PCR, and the respective size of each PCR product from each primer set. The nucleotide positions of each primer are indicated in parenthesis.

## Transformation into XL1-Blue

One 100  $\mu$ l aliquot of XL1-Blue competent cells was used for each transformation. Each ligation reaction was transformed into XL1-Blue cells and plated onto LB-ampicillin plates (200  $\mu$ g/ml ampicillin) using standard protocols as directed by "Molecular Cloning: A Laboratory Manual." (Sambrook and Russell, 2001).

## Overnight cultures of transformed bacteria

One 15 ml Falcon tube was labeled per colony, and 5 mls LB broth and 10 $\mu$ l Ampicillin (100 mg/ml) was added to each tube. Next, one colony was transferred to each

Falcon tube using a sterile pipette tip. The Falcon tube was then vortexed for 15 seconds and placed on a slanted rack overnight at 37°C.

### **Plasmid preps, analysis and sequencing**

Small scale plasmid purification was done for each sample using QIAprep® Spin Miniprep Kit (QIAGEN; Valencia, CA) as directed by manufacturer's instructions. Restriction digests of plasmids were performed using Eco R1 restriction enzyme to verify the presence of the PCR product prior to sending plasmid for sequencing. Samples were sent to the DNA Sequencing Core at the University of Michigan, Ann Arbor.

### **Real-time PCR using QuantiFast SYBR Green**

#### **Background and color (SYBR Green) calibration**

These steps were done following the manufacturer's instructions, using the plates provided for calibration (Eppendorf).

### **Real-time PCR optimization of GAPDH and astrocyte-specific genes**

#### **cDNA amount and final concentration optimization**

Suggestions were made for setting up real-time PCR reactions in Table 1 of QuantiFast SYBR Green PCR Handbook 01/2007 (QIAGEN). Using the parameters set in this table, a design was made for the initial reactions. These reactions and all subsequent real-time PCR reactions, were set up in 96-well plates that were labeled and stored in an ice box in the freezer. Keeping each reaction chilled on ice should prevent primer dimer formation and also keep the reagents non reactive. These reactions were

then set up in a Labconco PCR hood to prevent any contamination from entering our reactions. SYBR Green Master Mix was always half the total reaction amount and all other components were variable. cDNA amount did not exceed 10% (or 2.5 $\mu$ l) of the final reaction. Using this table, different  $\mu$ l volumes of each cDNA concentration ([cDNA]) were used to begin RT-PCR reactions including: 1  $\mu$ l [1:10], 2.5  $\mu$ l [1:10] and 1  $\mu$ l [1:4]. Next, 1  $\mu$ l of the upstream and downstream primers were added to each reaction to a final concentration of 1  $\mu$ M. Finally, RNase Free water was added to complete the reaction and to adjust the volume to 25  $\mu$ l. PCR programs were created for each set of reactions as directed by the Mastercycler ep *Realplex<sup>4</sup>* software manual (Eppendorf). Each gene was tested using the same sample cDNA. The reaction variation (Table 2) that gave the “best results” was used in subsequent optimization.

**Table 2: Reaction component variations used during optimization of real-time PCR primers**

<b>Reaction Components</b>	<b>Variation 1</b>	<b>Variation 2</b>	<b>Variation 3</b>
<b><math>\mu</math>l of [cDNA]</b>	1 $\mu$ l [1:10]	2.5 $\mu$ l [1:10]	1 $\mu$ l [1:4]
<b>SYBR Green</b>	12.5 $\mu$ l	12.5 $\mu$ l	12.5 $\mu$ l
<b>Up Stream Primer</b>	1 $\mu$ l [25 $\mu$ M]	1 $\mu$ l [25 $\mu$ M]	1 $\mu$ l [25 $\mu$ M]
<b>Down Stream Primer</b>	1 $\mu$ l [25 $\mu$ M]	1 $\mu$ l [25 $\mu$ M]	1 $\mu$ l [25 $\mu$ M]
<b>RNase-Free Water</b>	9.5 $\mu$ l	8 $\mu$ l	9.5 $\mu$ l
<b>Total</b>	25 $\mu$ l	25 $\mu$ l	25 $\mu$ l

Table 2: Reaction component variations 1-3 with variable volumes and concentrations of cDNA.

For every real-time PCR reaction two important plots were generated: the amplification plot and the melting curve. As the PCR program is taking place the Mastercycler ep *Realplex<sup>4</sup>* reads the fluorescence emitted from each reaction in real time and plots the amount of fluorescence verses either cycle number or time, for the amplification plot and subsequent generation of the melting curve (described below).

The amplification plot shows the fluorescence versus number of cycles. Real-time PCR products amplify in a particular manner, with three phases: exponential, linear and plateau (Figure 6). First, the exponential phase shows an increase in fluorescence in an exponential fashion, because no reagents are limiting at this point. The amount of fluorescence or PCR product can be associated with the starting number of mRNA transcripts (Yuan et al. 2006). With increasing cycles the PCR product increase is seen in a linear fashion, followed by a decline in the rate of increase (reagents are limiting) in the plateau phase (Yuan et al. 2006). Each amplification plot has a threshold level calculated by the software. We chose the default setting called the Noise Band, where the threshold level was calculated to be 10 standard deviations above the noise of the baseline (found in *Mastercycler ep Realplex<sup>4</sup>* manual by Eppendorf). The threshold level in Figure 6 is indicated with a bold horizontal line. The fluorescence of any sample crosses the threshold level at a particular cycle number during the exponential phase. The cycle number at which the threshold level is crossed is called the Ct value (Figure 6). The lower the Ct value is the more efficient the reaction parameter. A lower Ct value can also mean that there were a higher number of mRNA transcripts at the beginning of the reaction in samples (if the primers of a particular gene product were already optimized). Each reaction was set up in triplicate; thus, another aspect to consider is reproducibility. One has more confidence in choosing the optimal parameter based on lowest Ct value plus highest reproducibility.

**Figure 6: Amplification plot for real-time PCR reactions**

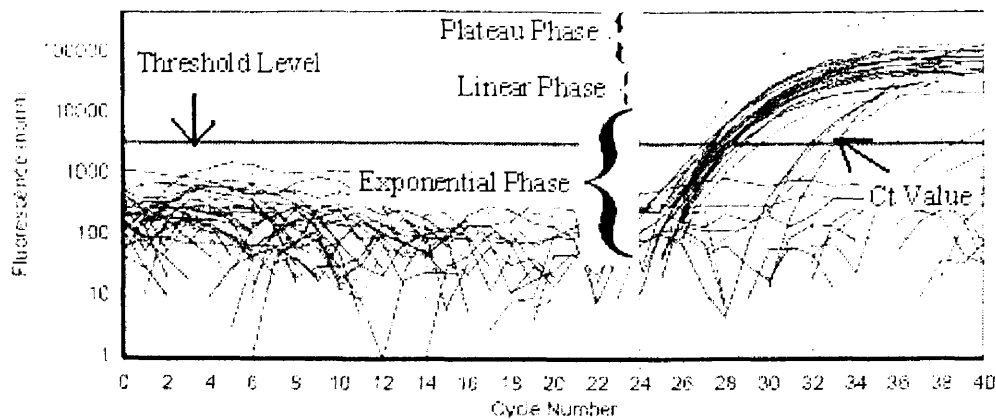


Figure 6: The Mastercycler ep *Realplex*<sup>4</sup> reads the log transformed fluorescence emitted from each reaction in real time and plots the amount of fluorescence versus cycle number in the amplification plot. The threshold level is indicated with a bold horizontal line. The Ct value is defined as the cycle number in which fluorescence of reaction products crosses the threshold level. The three phases (exponential, linear and plateau) are also indicated.

Melting curves were plotted by taking the first derivative of the dissociation curve by the software (generated by plotting fluorescence versus increasing temperature, causing the DNA to dissociate over time) and plotting this against temperature (Figure 7). The melting curve shows a spike indicating the temperature at which the amplified DNA dissociates. The temperature at which each PCR product dissociates is dependent upon its size and CG content. GFAP, S100, Vimentin and GAPDH PCR products are nearly the same size, so the higher the CG content of the PCR product the higher its melting temperature. Typical PCR product melting temperatures are relatively high and one peak should be seen in the melting curve (80-90°C). In contrast, primer dimer melting temperatures are relatively low (~60-75°C). If there is more than one peak, more than one PCR products are being amplified. Therefore, if there are primer dimers forming in

reactions at certain temperatures, the melting curve will reflect their presence. This is another factor that needs to be considered when evaluating the results of optimization. Overall, low Ct plus high reproducibility, along with a single peak in the melting curve, equals the optimal parameters (or “best results”). The optimal parameters found at each step in optimization were used in subsequent optimization steps.

**Figure 7: Melting curve for real-time PCR reactions**

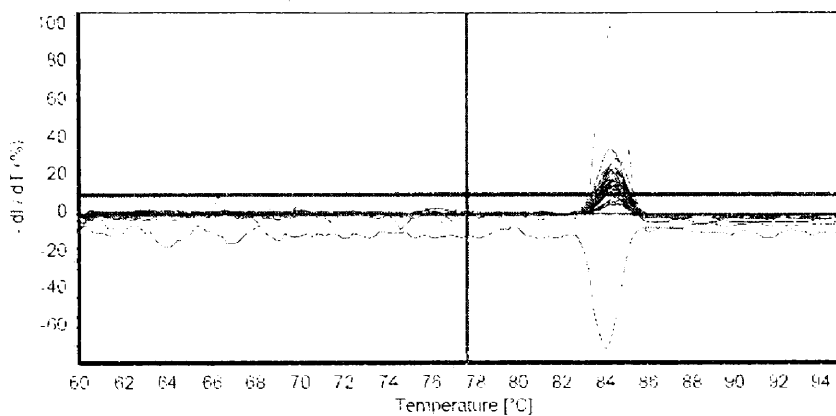


Figure 7: The melting curve is plotted by taking the first derivative of the dissociation curve and plotting that versus temperature. This shows which temperature the DNA amplified in the reaction dissociates.

### **Temperature optimization**

Suggestions for temperature optimization were found in “Optimization of the new Lambda Primers-Gradient PCR” (Eppendorf). A gradient of annealing temperatures was set up across the 12 columns of a plate layout (Table 3). Each reaction was identical, and each temperature had triplicate reactions plus one No Template Control (NTC). Each gene was tested for best results using the same sample cDNA and same temperature gradient found in identical PCR programs. Each PCR program started with an initial 5 minutes at 95°C to activate the DNA polymerase in the SYBR Green QuantiFast Master



Mix. This is followed by 40 cycles of denaturing (95°C) for 15 seconds, annealing (gradient as indicated by Table 3) for 15 seconds and extension (72°C) for 20 seconds. After amplification, the reactions were subjected to melting curves. The annealing temperature that gave the “best results” was used in subsequent optimization.

Well Position	1	2	3	4	5	6	7	8	9	10	11	12
Annealing Temperature Celsius	49.9	50.2	50.9	52.0	53.4	54.9	56.5	58.1	59.5	60.7	61.6	62.0

Table 3: The gradient of annealing temperatures across the 12 columns used to optimize all genes.

### **Primer concentration optimization**

Next, different combinations of final primer concentrations were optimized. Suggestions for primer optimization were found in “Optimization of the new Lambda Primers-Gradient PCR” (Eppendorf). All combinations of final upstream verses downstream primer concentrations are shown in Table 4: each combination was tested in triplicate. These triplicate reactions were set up by adding 1 µl of 6.25 µM, 12.5 µM and 25 µM primer concentrations into the 25 µl reactions, which gave final concentrations of 250 nM, 500 nM and 1000 nM respectively (Table 5). A total of nine different combinations of upstream verses downstream final primer concentrations were examined for each gene. Next, NTC reactions were set up in triplicate for each 250/250, 500/500 and 1000/1000 combinations. Each gene was tested for optimal results using the same sample cDNA. The primer concentration that gave the “best results” was used in subsequent standard or efficiency curves. Optimal parameters were found for each gene (Table 6).

**Table 4: Matrix of final upstream versus downstream primer concentration**

		Upstream primer concentrations		
		250 nM	500 nM	1000 nM
Downstream primer concentrations	250 nM	250/250	500/250	1000/250
	500 nM	250/500	500/500	1000/500
	1000 nM	250/1000	500/1000	1000/1000

Table 4: This matrix of final upstream versus downstream primer concentration shows each combination used for all each gene during primer optimization.

**Table 5: Reaction components used during primer concentration optimization**

Reaction Components	Volume and [Concentration]
$\mu\text{l}$ of [cDNA]	1 $\mu\text{l}$ [1:4]
SYBR Green Master Mix	12.5 $\mu\text{l}$
Up Stream Primer	1 $\mu\text{l}$ [6.25 $\mu\text{M}$ , 12.5 $\mu\text{M}$ or 25 $\mu\text{M}$ ]
Down Stream Primer	1 $\mu\text{l}$ [6.25 $\mu\text{M}$ , 12.5 $\mu\text{M}$ or 25 $\mu\text{M}$ ]
RNase-Free Water	9.5 $\mu\text{l}$
<b>Total</b>	25 $\mu\text{l}$

Table 5: Each reaction was set up using the same volume of reaction components. The concentration of all reaction components were equal except for upstream and downstream primer concentrations. These varied between 6.25 $\mu\text{M}$ , 12.5 $\mu\text{M}$  and 25 $\mu\text{M}$ .

**Table 6: Optimal parameters for each gene**

Gene	Optimal cDNA (uls and dilution)	Optimal Annealing Temperature( $^{\circ}\text{C}$ )	Optimal Final [Primer] Up:Down
<b>GFAP</b>	1 $\mu\text{l}$ [1:4]	53.5	250 nM: 500 nM
<b>S100</b>	1 $\mu\text{l}$ [1:4]	58.0	500 nM: 1000 nM
<b>Vimentin</b>	1 $\mu\text{l}$ [1:4]	53.5	500 nM: 1000 nM
<b>GAPDH</b>	1 $\mu\text{l}$ [1:4]	56.5	1000 nM: 1000 nM

Table 6: Results of volume and [cDNA], temperature and [primer] optimization for each gene.

### Standard and efficiency curves

Standard curves are important for determining PCR efficiency and are done for standard or reference genes (i.e., GAPDH). Efficiency curves are essentially equal to

standard curves, but are done for all experimental genes. Each standard and efficiency curve was done twice: once for a cDNA sample from the wild type animals and then for cDNA from Pde6b- animals. Five 10-fold serial dilutions were prepared from the cDNA stock (considered to be the 1x concentration); reactions were carried out in triplicate for each dilution. These curves were plotted as Ct versus  $\text{Log}_2[\text{cDNA}]$ , which can be used to estimate the efficiency of each PCR product being amplified (Yuan et al., 2006). Theoretically, the number of PCR products should be doubled each amplification cycle, which would lead to percent amplification efficiency (PAE) equal to 100% (Yuan et al., 2007). This would correspond to amplification efficiency (AE) of 2, calculated by the equation  $2^{\text{PAE}}$  (Yuan et al., 2007). The reality of AE and PAE for a given sample is that they may not be optimal, depending on a number of criteria: optimal [primer], optimal annealing temperature, pipetting error, etc. (Yuan et al., 2007). PAE was found for every gene by taking the  $-(\text{slope})$  of the regression line fit to the curve data for that gene.

The regression line should have a slope close to -1 and a high r squared value, where  $\text{PAE} = -(\text{slope})$  (Yuan et al. 2007). These regression lines were then tested for significance based on two criteria. First, the slope of each line should not be significantly different from -1. Second, the Pde6b- and Pde6b+ lines should not be significantly different from each other for the same gene (Yuan et al. 2006). If both of these criteria were met, the efficiency values were accepted to be optimal. If these criteria were not met, the value for PAE was used as a correction term for the raw data.

Prior to each reaction set up, a Plate layout and PCR program was set up according to the Mastercycler *Realplex*<sup>4</sup> manual (Eppendorf). Next, a master mix was made for the 15 reactions (3 reactions per [cDNA]). The tube for the reaction mix was

labeled, wrapped in aluminum foil, and placed on ice. The reaction master mix was made by adding 187.5  $\mu$ l of SYBR Green Master Mix, 142.5  $\mu$ l RNase-free Sterile Water, 15  $\mu$ l upstream primers, and 15  $\mu$ l downstream primers together and mixed by pipetting up and down. This mixture was kept on ice while adding 1  $\mu$ l of the appropriate [cDNA] to each well. 24  $\mu$ l of the reaction master mix was then added to each well and mixed by pipetting up and down (Note: the tube was held with thumb and index finger near the top of the tube to keep the reaction mix from warming up). Strip caps were placed over reaction wells and wiped off with a Kim wipe. This plate of reactions was then placed in the Mastercycler *Realplex<sup>4</sup>*, the lid closed, and the PCR program initiated.

At the end of the reactions the data for each curve were then prepared for evaluation. Triplicate data were collected and only one value was needed, so the mean was taken of the closest two Ct values (within one amplification cycle), leaving one value for each [cDNA]. These data (see Appendix 1) were next analyzed using SPSS by simple linear regression models and 95% confidence intervals (Syntax found in Appendix 3) to test if the slopes of the lines were the same as -1, and to test if the lines for each gene are the same between genotypes (Output found in Appendix 2). If the slopes of these lines are significantly different from -1 and significantly different from each other, a correction factor, PAE, should be used in subsequent analysis.

### **Real-time PCR procedure for individual runs**

All cDNA samples (1:4 concentration) were subjected to identical real-time PCR for each gene in triplicate. 1.5 ml microcentrifuge tubes were labeled for each gene as a master mix tube, wrapped in tin foil and placed on ice in the hood. Pipettes, pipette tips, ultra clear strip caps, empty master mix tubes (on ice) and waste container was placed in

the hood and sterilized by turning on the UV light for 15 min. The reagents were prepared by centrifuging the primers, cDNA and SYBR green (wrapped in aluminum foil). Next, the primers and SYBR green were vortexed for 15 seconds, then gently tapped on the counter top to move all liquid to the bottom of the tubes.

Appropriate real-time PCR programs were constructed on Mastercycler *Realplex*<sup>†</sup>. These PCR programs were similar to previous programs (Figure 7), but they had a specific temperature gradient so that all four genes could be run together (Table 7), with each subjected to their optimal annealing temperature. Two cDNA samples were run together: one Pde6b+ and one Pde6b- (Figure 8). I was kept blind to the age and genotype of all animals, so Dr. Jarvinen told me which pairs of cDNA samples to run together. (Note that for regular maintenance the computer was restarted for 10 minutes after several Real-time PCR runs).

<b>Table 7: Gradient of annealing temperatures used for data collection runs</b>												
<b>Column Number</b>	1	2	3	4	5	6	7	8	9	10	11	12
<b>Annealing Temperature Celsius</b>	53.4	53.5						56.5				58.1

Table 7: A gradient was used for annealing temperatures resulting in the optimal annealing temperature for each gene in the wells indicated above (column 1: GFAP; column 2: Vimentin; column 8: GAPDH and column 12: S100). Only relevant temperatures are indicated.

The Plate layouts were created next. Three wells were chosen, labeled as appropriate (unknown or standard, Name: Gene name + cDNA and Target 1: Gene) for each gene and cDNA sample, and grouped as replicates. These files were saved as assays with appropriate information in the saved name (cDNA samples used, Run # and Date).

The reactions were set up by adding the following to each tube: 58  $\mu$ l RNase free water, 75  $\mu$ l Quantifast SYBR Green, 6  $\mu$ l Up stream primer and 6  $\mu$ l Down stream primer (new pipette tips were used for each amount of reagent added). The master mix tubes were centrifuged at maximum speed for 30-45 seconds to mix and placed back on ice. Next, 1  $\mu$ l of 1:4 cDNA was added to wells for each gene in triplicate (6 wells total) (Figure 8 step 1). This was repeated for the 2<sup>nd</sup> cDNA (12 wells total) (Figure 8 step 2). Precautions as described for standard and efficiency curves were also followed here. Then 24  $\mu$ l of master mix were added to each well for the appropriate gene (Figure 8 steps 3-6) using a new tip for every addition and pipetting up and down several times to mix reactions well.

**Figure 8: Real-time PCR reaction set up in a 96-well plate for individual runs**

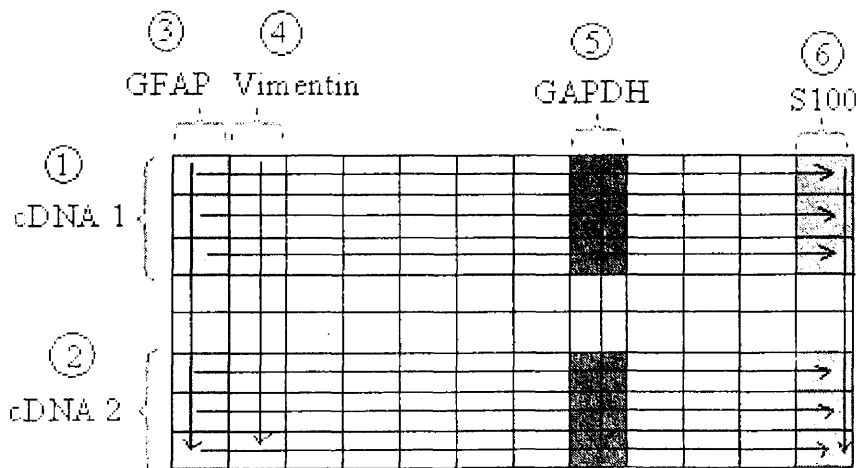


Figure 8: This drawing represents the 96 well plate and the exact set up for each of the real-time PCR runs. The numbers indicated here show the order/step number for the addition of each reaction component (as described above).

When all reactions were ready, they were covered with ultra clear strip caps. The plate was put into the Mastercycler *Realplex*<sup>4</sup> and the strip caps were wiped with a Kim wipe. The lid was closed, the handle pulled down and the program was started when the

light on the Mastercycler *Realplex<sup>4</sup>* turned green. When the reactions were complete the data analysis was done.

### **Data analysis criteria**

The data were obtained in triplicate. However, for subsequent analysis, only two data points were needed. Criteria were established to eliminate the outlier without bias so that the best two Ct values would be kept. The criterion was to accept the 2 closest of the triplicate values, as long as they were within one amplification cycle. This becomes an accepted duplicate pair that is segregated into high and low Ct values ( $R_{High}$  and  $R_{Low}$ ). If the data did not meet the criteria, they were repeated more than once. Triplicates that were repeated had to meet the first criteria plus be reproducible. This meant that at least two repeat triplicate reactions must meet the first criteria plus the average of those accepted duplicates must be within one amplification cycle of each other. If these two repeated accepted duplicates were not within one amplification cycle, another accepted duplicate was required. When three accepted duplicates were obtained, the median duplicate was accepted at the valid Ct for that sample.

These data were then tested for correlation between same age and genotype for each gene. This study sampled Pde6b- and Pde6b+ mice at 10 different time points with three mice per time point (5 mice for each genotype for PND 100). The sample size was 6 (or 10) for each age. We expected that the Ct values would be similar for all animals at the same age for the same gene. The outputs for each correlation test are found in Appendices 6-9 and the SPSS syntax is Appendix 10.

Next, the data were analyzed using a relative quantification method called  $\Delta Ct$ . This method takes the difference between Ct values of the target (astrocytes-specific) and

reference (GAPDH) genes, which compares the expression of the target and reference gene (Yuan et al., 2006). The  $\Delta Ct$  method uses the equation:  $\Delta Ct = Ct_{\text{target}} - Ct_{\text{reference}}$ . Here, the reference gene Ct value was always lower than the target gene Ct value. This is because number of mRNA molecules is always higher for the reference gene, GAPDH. The average  $\Delta Ct$  was then taken for the three values in each unique genotype/age. Next, each gene's  $\Delta Ct$  values were plotted versus age for both genotypes. This gave two lines for each gene: Pde6b<sup>-</sup> versus Pde6b<sup>+</sup>. Thus, our gene expression can be interpreted easily between genotypes.



## **Chapter Three: Results**

### **Standard and efficiency curves analysis**

The standard and efficiency curves were tested using a simple linear regression analysis and confidence intervals (shown in Graph 2). Remember, we are trying to find out if the slopes of these lines are significantly different from -1 and if the lines for each gene are significantly different between genotypes. It was found (regression analysis syntax 3) that the Pde6b<sup>-</sup> lines were not significantly different from the Pde6b<sup>+</sup> lines for any gene indicated by insignificant P values ( $P > 0.05$ ) (Table 8). Confidence intervals were used to test if the slopes of each of the regression lines were the same or different from -1. If the confidence intervals included -1, there was statistical evidence in favor of the hypothesis that the slope is equal to -1 for that genotype. If the confidence intervals did not include -1, there was evidence that the slope was different from -1 for that particular genotype. It was found that the slopes of each of the regression lines were not significantly different from -1 with the exception of GFAP and vimentin for Pde6b<sup>-</sup> mice (Table 8). Although this was found, PAE will not be used in subsequent analysis. The rationale behind this decision will be discussed later.

### **Raw data analysis using correlation**

Ct data were subjected to a correlation test. Remember, each age of mice had a sample size of 6 (3 Pde6b<sup>-</sup> and 3 Pde6b<sup>+</sup>), or 10 for PND 100. The high and low Ct values for each mouse of the same age were plotted together on a scatter plot, where the X value was the high Ct and the Y value was the low Ct. All of the high and low Ct values for the mice of the same age correlated significantly: every correlation model had

high r values and showed significant correlation at the 0.01 level, with the exception of two groups with significance at the 0.05 level and one group with marginal significance (where P = 0.58 for GAPDH at PND 42) (Table 9). These results indicate that we have found valid high and low Ct values from each of the mice at each age.

**Table 8: Regression analysis and confidence interval values**

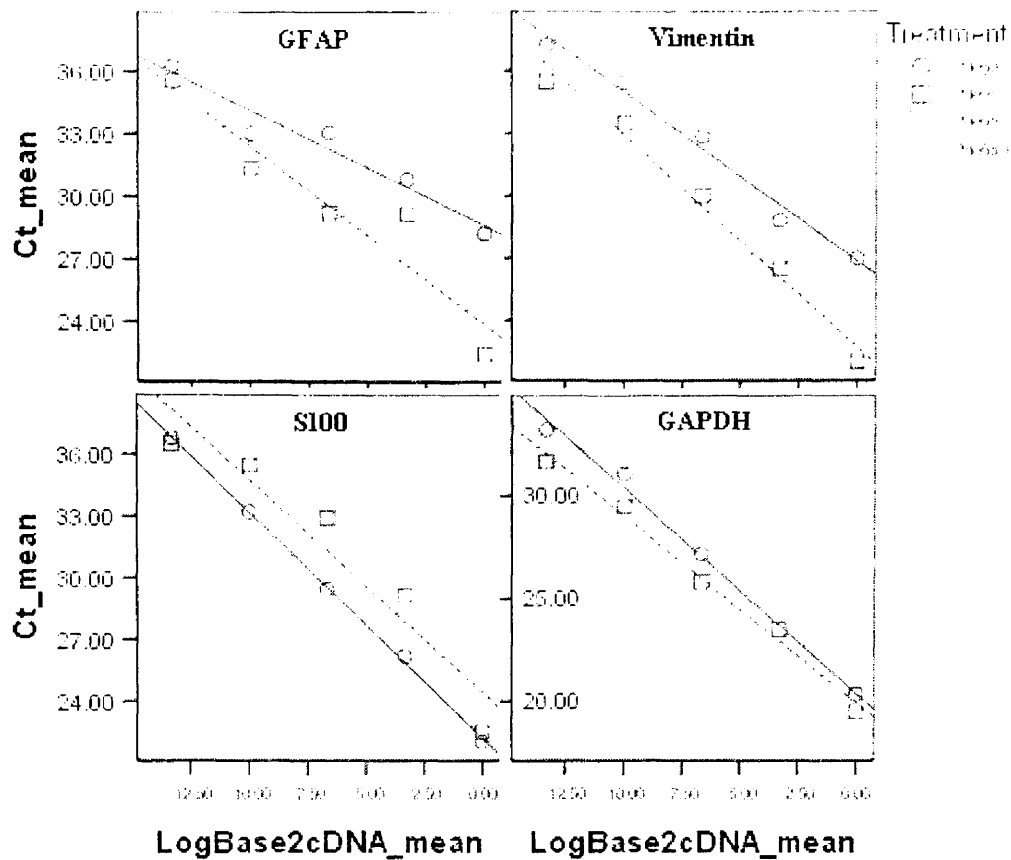
Gene	Pde6b- mice	Pde6b+ mice	P value
GAPDH	-1.002 (-1.125, -0.878)	-0.912 (-1.035,-0.788)	0.252
GFAP	-0.548 ( <b>-0.872, -0.225</b> )	-0.854 (-1.178,-0.530)	0.154
S100	-1.099 (-1.421, -0.778)	-1.034 (-1.358,-0.713)	0.738
Vimentin	-0.815 ( <b>-0.990, -0.640</b> )	-1.025 (-1.200,-0.850)	0.084

Table 8: Slope (95% confidence intervals) and P values from regression analysis are summarized here for each unique age/genotype. Confidence intervals for every unique genotype/age include -1 with the exception of the bold face values (GFAP and vimentin of Pde6b- mice). P values indicate the level of significance for the similarity between the two regression lines (one for each genotype) for each gene. Each gene showed a P value higher than 0.05 indicating that there is no significant difference between regression lines for each genotype.

### **ΔCt data analysis using parametric and non-parametric tests**

The ΔCt data (Appendix 10) were subjected to analysis for differences in gene expression at various ages for each gene. Since there is a sample size of three for each unique genotype/age, a mean was taken. This left only one ΔCt value for wild type and retinal degeneration at every time point for each gene. These values were plotted over time for GFAP (Graph 3), S100 (Graph 4) and vimentin (Graph 5) so that each gene's expression pattern changes over time between genotypes could be seen (syntax for graphing in Appendix 13).

**Graph 2: Scatter plot of standard and efficiency curves with regression lines**



Graph 2: Standard and efficiency curves for Pde6b- and Pde6b+ mice with their respective regression lines for each gene. Regression analysis using confidence intervals shows that all lines are not significantly different from  $-1$  and lines of the same gene do not differ from each other.

Next, both parametric and non-parametric tests were done to examine for significant differences between the  $\Delta Ct$  values of each gene between genotypes for each age point. First, a parametric test was done (the T-test; syntax and output in Appendices 11-12, respectively), followed by a non-parametric test (Kruskal-Wallis Test; syntax and output in Appendices 14-15, respectively). These tests gave identical results where significant differences were seen (Graphs 3-5). In fact, each significant difference seen at

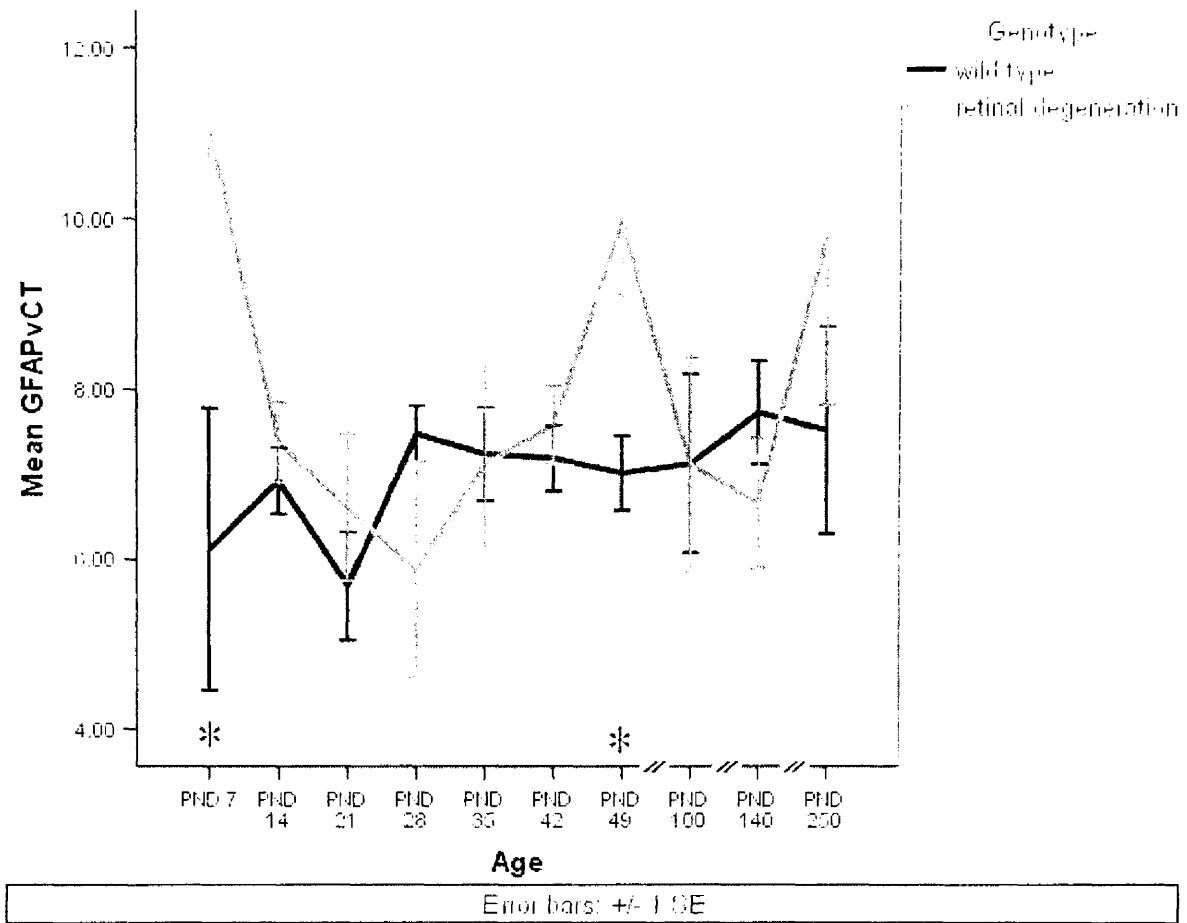
Table 9: Correlation summary: r values and significance levels for each unique gene age

Age	Gene Product			
	GFAP	S100	Vimentin	GAPDH
PND 7	.999	.972	.990	.991
PND 14	.844**	.911**	.962	.998
PND 21	.935	.996	.961	.941
PND 28	.997	.969	.978	.990
PND 35	.997	.995	.997	.997
PND 42	.976	.992	.960	.797*
PND 49	.992	.998	.997	.997
PND 100	.994	.991	.990	.997
PND 140	.984	.991	.987	.986
PND 250	.996	.986	.997	.991

Table 9: GFAP, vimentin, S100 and GAPDH r values for correlation models done at each of the 10 ages in our study. All data were found to correlate significantly at the 0.01 level (two-tailed) except for those indicated by asterisks (\*\* Correlate significantly at the 0.05 level (2-tailed); \* Correlation is marginally significant at the 0.051-0.06 level (2-tailed)). These results indicate that we have found valid high and low Ct values from each of the mice at each age.

a given time for a given gene was in favor of higher gene expression in wild type animals. Therefore, less mRNA transcripts were being expressed in retinal degeneration mice than in wild type mice. This means that it would take more amplification cycles for a particular gene to reach the threshold level in retinal degeneration mice compared to wild type mice. Graphically, this is seen by a higher  $\Delta C_t$  value for retinal degeneration mice compared to wild type mice at that time for that particular gene. GFAP expression at PND 7 and 49 was found to be significantly higher in wild type mice compared to retinal degeneration mice (Graph 3). S100 expression at PND 49 was significantly higher in wild type mice compared to retinal degeneration mice (Graph 4). Vimentin expression at PND 21 was found to be significantly higher in wild type mice than retinal degeneration mice (Graph 5). Thus, GFAP is expressed less in RD at PND 7, Vimentin is expressed less in RD at PND 21, and both GFAP and S100 are expressed less in RD at PND 49 (Graphs 3-5).

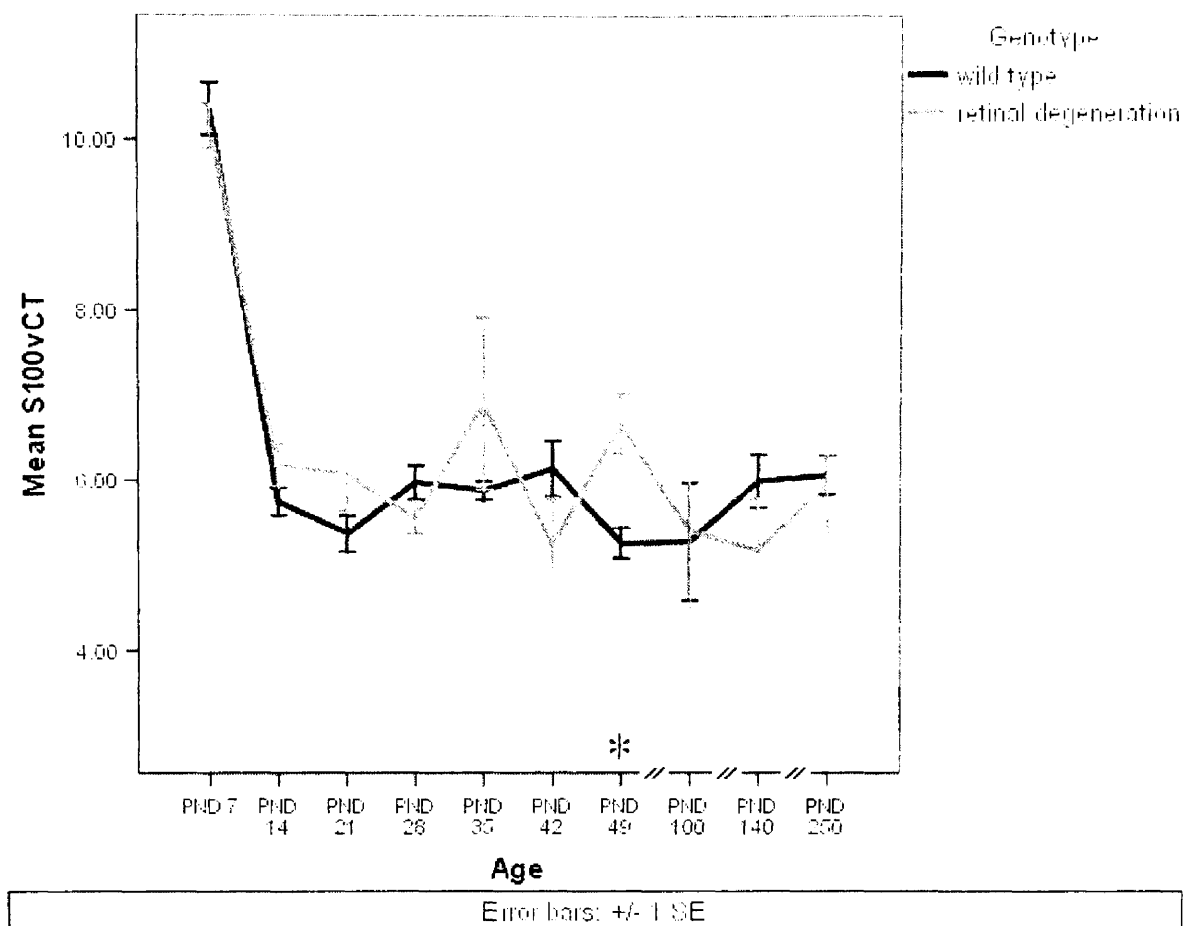
**Graph 3: Mean GFAP  $\Delta$ Ct for wild type and retinal degeneration over time**



\* Significant at the 0.05 level (2-tailed).

Graph 3: Mean GFAP  $\Delta$ Ct (GFAPvCT) was taken for each age and genotype and plotted together (plus error bars). Significance was found (indicated by an asterisk) for differences in gene expression of GFAP between genotypes of each age group. Two tests were done to test for significant differences: a parametric (T-test) and non-parametric (Kruskal-Wallis Test) analysis. Levels of GFAP mRNA expression were significantly higher in wild type compared to RD mice at PND 7 and 49, as shown by the mean  $\Delta$ GFAP Ct values at these time points. Unequal distances between tick marks are indicated by slash marks (/).

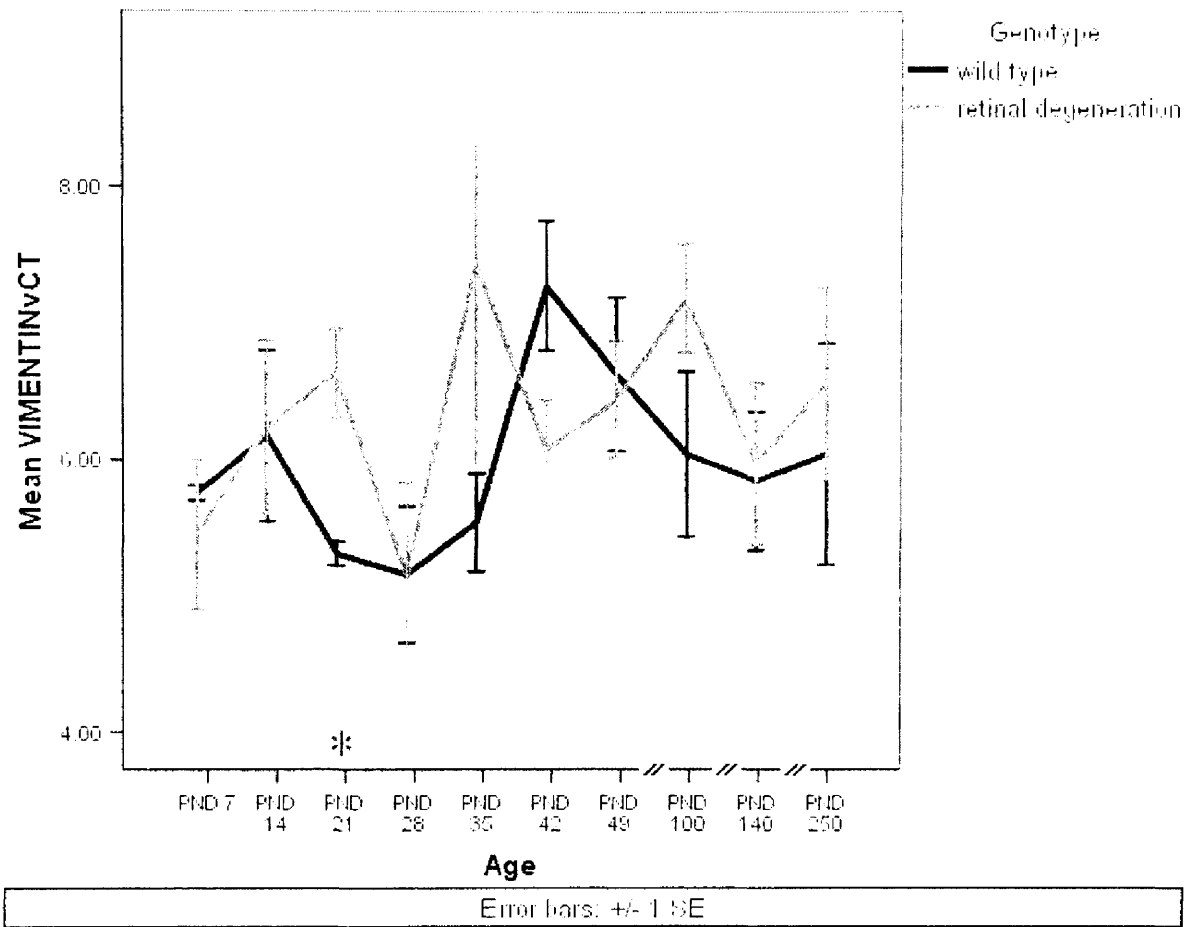
**Graph 4: Mean S100  $\Delta$ Ct for wild type and retinal degeneration over time**



\* Significant at the 0.05 level (2-tailed).

Graph 4: Mean S100  $\Delta$ Ct (S100vCT) was taken for each age and genotype and plotted together (plus error bars). Significance was found (indicated by an asterisk) for differences in gene expression of S100 between genotypes of each age group. Two tests were done to test for significant differences: a parametric (T-test) and non-parametric (Kruskal-Wallis Test) analysis. Levels of S100 mRNA expression was significantly higher in wild type compared to RD mice at PND 49, as shown by the mean  $\Delta$ S100 Ct values at this time point. Unequal distances between tick marks are indicated by slash marks (/).

**Graph 5: Mean vimentin  $\Delta$ Ct for wild type and retinal regeneration over time**



\* Significant at the 0.05 level (2-tailed).

Graph 5: Mean vimentin  $\Delta$ Ct (VIMENTINvCT) was taken for each age and genotype and plotted together (plus error bars). Significance was found (indicated by an asterisk) for differences in gene expression of vimentin between genotypes of each age group. Two tests were done to test for significant differences: a parametric (T-test) and non-parametric (Kruskal-Wallis Test) analysis. Levels of vimentin mRNA expression was significantly higher in wild type compared to RD mice at PND 21, as shown by the mean vimentin  $\Delta$ Ct values at this time point. Unequal distances between tick marks are indicated by slash marks (/).

## Chapter Four: Discussion

### Raw data analysis

We used astrocyte-specific genes to examine changes in expression in the visual cortex of Pde6b<sup>-</sup> (RD) and Pde6b<sup>+</sup> (WT) mice. As mentioned previously, 28% of the cells in the visual cortex are astrocytes. The results of the mean  $\Delta C_t$  analysis (parametric and non-parametric tests for significance) show that GFAP is expressed less in RD mice at PND 7, vimentin is expressed less in RD mice at PND 21, and both GFAP and S100 are expressed less in RD mice at PND 49 (relative to WT in all cases)(Figure 9).

**Figure 9: Pde6b<sup>-</sup> (RD) mouse behavior and gene expression time-line**

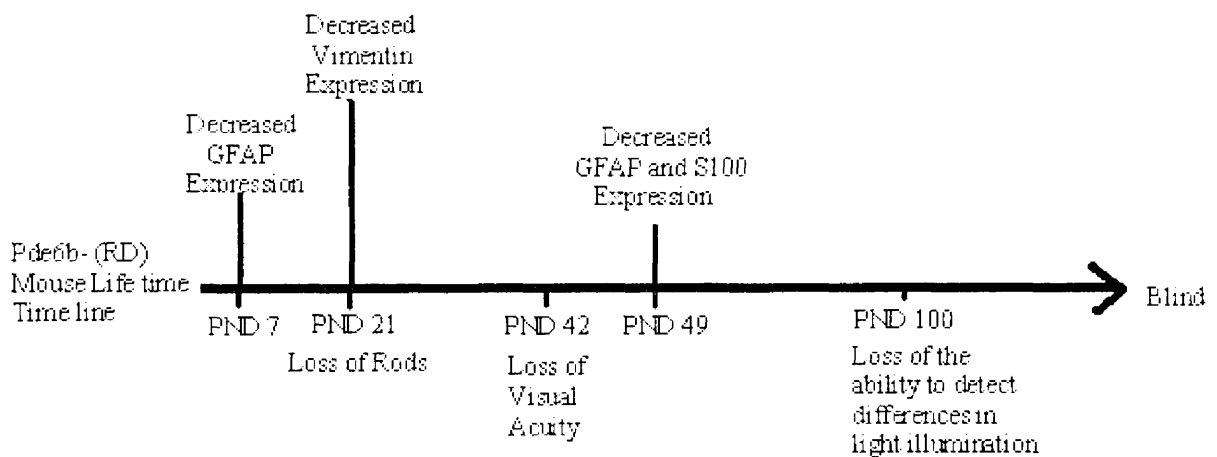


Figure 9: Time-line summary of astrocyte-specific gene expression and behavior changes seen in Pde6b<sup>-</sup> mice. Significance was found using parametric and non-parametric tests. GFAP is expressed less in RD at PND 7, vimentin is expressed less in RD at PND 21, and both GFAP and S100 are expressed less in RD at PND 49 (based on comparison to Pde6b<sup>+</sup> mice data) (indicated above time line). These ages are on or near relevant ages PND 21, 42 and 100 when important aspects of vision are lost (indicated below time line).

The first time point to show a significant difference between WT and RD mice was at PND 7, where GFAP expression is less in RD mice. This age was not of critical



importance from our behavioral studies, and is prior to mice opening their eyes at PND 12 (Hooks and Chen., 2007). However, PND 7 is within the critical period for ocular dominance plasticity (ODP) in the visual cortex of mice (Hooks and Chen., 2007). It was found that OD columns are formed for the most part prior to visual stimulation: neural connections are established before eye opening and refined in response to visual experience (Hooks and Chen., 2007). Pde6b<sup>+</sup> mice show a relatively moderate level of GFAP expression (Graph 3), which could help stabilize the neural connections already made in the OD columns of the visual cortex during normal development. Pde6b<sup>-</sup> mice, however, have a much lower level of GFAP expression and may be experiencing less than normal OD column development (i.e., a delay in ocular dominance column development). A delay in OD column development could explain why GFAP expression is low in Pde6b<sup>-</sup> at PND 7, since the visual cortex in these mice at PND 7 might need to continue to be plastic. This is supported by our data showing high expression of vimentin at PND 7 in Pde6b<sup>-</sup> mice (Graph 5). This delay in development is only for a short period and is followed by an increase in GFAP expression peaking at PND 28 (the peak of ODP). An explanation for this rebound of GFAP expression in Pde6b<sup>-</sup> mice could be that the OD columns' development is complete and the neural connections made are being stabilized by GFAP-expressing astrocytes.

The second time point to show a significant difference between WT and RD mice was at PND 21, where vimentin expression is less in RD mice. This age is when rods are lost in Pde6b<sup>-</sup> mice (Marc et al., 2003; Chang et al., 2002), and a low level of vimentin expression does not make sense. Over time we see that Pde6b<sup>-</sup> and Pde6b<sup>+</sup> mice show relatively high levels of vimentin expression at PND 7 followed by decrease in

expression by PND 14 (Graph 5). Vimentin expression in Pde6b<sup>+</sup> mice then increases by PND 21 (Graph 5), which could be due to normal cues during development to increase plasticity. Vimentin expression in Pde6b<sup>-</sup> mice, on the other hand, continues to decrease until PND21, which could be explained by the loss of rod function by PND 21 (Graph 5). The normal developmental cues to increase plasticity in the visual cortex may not be present in the Pde6b<sup>-</sup> mice, which could block an increase in vimentin expression. Pde6b<sup>-</sup> vimentin expression does increase to wild type levels by PND 28 (Graph 5) possibly because the cue for an increase in vimentin expression came a week late.

The third time point to show a significant difference between WT and RD mice was at PND 49. The behavioral tests suggest that PND 49 is immediately after visual acuity is lost (by PND 42) and well before the ability to detect differences in light illumination lost (by PND ~100). Thus, PND 49 is between two very important ages where the mice are in the process of losing the function of their cones. This age is where our data show a decrease in gene expression for GFAP and S100. Remember that GFAP and S100 expression are correlated, and these proteins are seen in mature astrocytes. At PND 49 cone function is degrading and the neural connections previously made with cones are most likely no longer useful. New neural connections may be made by remodeling, which would require an increase in plasticity via an increase in vimentin expression. Vimentin expression is seen to increase from PND 42 to PND 100 (Graph 5). PND 49 is during cone degradation and one should expect an increase in plasticity so that the brain can remodel and this is reflected in our data.

These Pde6b<sup>-</sup> and Pde6b<sup>+</sup> mice are going through many changes developmentally. It was hypothesized earlier that we would find astrocyte-specific gene

expression pattern changes at PND 21, 42 and 100 in astrocytes of the visual cortex in our Pde6b<sup>-</sup> mice compared to Pde6b<sup>+</sup> mice. In summary, our data suggest that changes in gene expression are taking place in some way at PND 7, 21 and 49. Our hypotheses may not be fully supported at the specific ages we found to be important via behavioral tests; however, our data do suggest changes in gene expression at potentially relevant ages (PND 7, 21 and 49).

Although this data is important for developing further research plans, the data obtained here is limited. Ct values are reflecting relative mRNA expression levels in the visual cortex of the mice. This is not at the protein level, which is much more important to consider. Overall, the conclusions made here are important, they are not fully supported by the data because we measured mRNA expression

The correlation tests support that the raw data obtained here were valid for each of the mice at each age. Each set of data had a sample size of 6. All sets of data showed significant correlation (high r values and significance at the 0.05 level), with the exception of one marginally significant group (GAPDH at PND 49) (Table 8), even with our small sample size. Again, these results indicate that we have found legitimate high and low Ct values from each of the mice at each age.

### **Standard and efficiency curves analysis**

The main purpose for standard and efficiency curves is to be able to use these data for statistical treatments (Yuan et al. 2006). Each curve gives a measure of efficiency, which can be used to support the raw data obtained or used as a correction term. Many studies to date do not measure levels of efficiency (Yuan et al. 2006), and this can be

problematic. The data measurement in real-time PCR is Ct, a measure obtained during the exponential phase of amplification. The Ct value is indirectly proportional to the number of mRNA transcripts in a starting sample. If the efficiency of gene A is 100% and the efficiency of gene B is 80%, this difference in efficiency will have an exponential effect on the fluorescence detected and, therefore, the Ct value. I will illustrate this with an example, in which one cDNA sample is used for genes A and B. This cDNA has the same number of starting mRNA transcripts, 10, for each gene. If reagents were not limiting during the first 20 amplification cycles, then each reaction should increase exponentially at their respective efficiency levels. At the end of 20 cycles gene A, with an efficiency level of 100%, now has  $2^{1.00 * 20 \text{ cycles}} = 1,048,576$  copies of gene product A. At the end of the same 20 cycles gene B, with an efficiency level of 80%, now has  $2^{0.80 * 20 \text{ cycles}} = 65,536$  copies of gene product B. This is only 6.25% of gene product A!

We also considered how efficiency impacts Ct. Returning to the above example, assume the gene product A fluorescence was high enough at 20 cycles to pass the threshold level, and it thus has a Ct of 20. Gene product B has not crossed the threshold level yet. How many cycles will it take for gene product B to reach a fluorescence comparable to 1,048,576 copies? To find this out we can set 1,048,576 equal to  $2^{0.80 * n \text{ cycles}}$ , and solve for cycle number, n. Our Ct value for gene product B with an efficiency value of 80% is 25. Thus, an efficiency value of 80% dramatically changed the Ct value for gene B, even though it started with an equal number of mRNA transcripts. This example clearly illustrates why efficiency values are important during statistical treatments.

It was found that the standard and efficiency curves for each gene were not significantly different from each other. It was also found that the slopes of each line were not significantly different from -1. However, the small sample size casts these results into some doubt. There were only two different samples used to get the standard and efficiency data, one of each genotype of the same age (PND 100). With such a small sample size, the standard error skyrockets. This could beg the question “how could the slopes of these lines be different from -1?” With a slightly higher number of samples being used for the curve data, the seemingly different trends would most likely become significant. A good example of this can be seen in the efficiency curves of GFAP. These lines seem to show slopes that could be different from each other. If there were even a couple more samples indicating this pattern of difference between the slopes of regression lines of Pde6b- verse Pde6b+, there would most likely be a significant difference.

Finally, it would be a good idea to include at least one sample from each age and genotype for the standard and efficiency curves. This would take much more time and energy, but would give a better indication if a correction factor should be used. Also, using a correction factor here would seem reasonable at another level. Our standard and efficiency curves were measured from one age (PND 100). How could a correction term derived from one age be the representative for all other ages? In the future, standard and efficiency curves should be done for every age and genotype. This would test whether efficiency is high enough to accept the raw data or if one age/genotype has lower PAE, it could be corrected for.

## Literature Cited

- Argandona, E.G., Rossi, M.I., and Lafuente, J.V. "Visual deprivation effects on the S100 $\beta$  positive astrocytic population in the developing rat visual cortex: a quantitative study." Developmental Brain Research 141 (2003): 63-69.
- Blumer, K.J. "Vision: The need for speed." Nature 427 (2004): 20-21.
- Chang, B., Hawes, N.L., Hurd, R.E., Davisson, M.T., Nusinowitz, S., Heckenlively, Jr.R. "Retinal degeneration mutants in the mouse." Vision Research 42 (2002): 517-525.
- Dahl, D., Rueger, D.C., Bignami, A., Weber, K. and Osborn, M. "Vimentin, the 57,000 molecular weight protein of fibroblast filaments, is the major cytoskeletal component in immature glia." European Journal of Cell Biology 24(2) (1981): 191-196.
- Donato, R. "Intracellular and Extracellular roles of S100 proteins." Microscopy Research and Technique 60 (2003): 540-551.
- Eng, L.F., Ghirnaikar, R.S., Lee, Y.L. "Glial fibrillary acidic protein: GFAP-thirty-one years. (1969-200). Neurochemistry Research 25 (2000): 1439-1451.
- Gabbott, P.L. and Stewart, M.G. "Distribution of neurons and glia in the visual cortex (area 17) of the adult albino rat: a quantitative description." Neuroscience 21(3) (1987): 833-845.
- Goldman, R.D., Khuon, S., Chou, Y.H., Opal, P. and Steinert, P.M. "The function of intermediate filaments in cell shape and cytoskeleton integrity." Journal of Cell Biology 134 (1996): 971-983
- Gordon, J.A. "Cellular mechanisms of visual cortical plasticity: A game of cat and mouse." Learning and Memory 4 (1997): 245-261.
- Hooks, B.M. and Chen, C. "Critical periods in the visual system: changing views for a model of experience-dependent plasticity." Neuron 56 (2007): 312-326.
- Hubener, M. "Mouse visual cortex" Current Opinions in Neurobiology 13 (2003): 413-420.
- Ionita, M.A. and Pittler, S.J. "Focus on the molecules: rod cGMP phosphodiesterase type 6." Experimental Eye Research 82 (2007): 1-2.
- Jones, B.W. and Marc, R.E. "Retinal remodeling during retinal degeneration." Experimental eye research 81 (2005): 123-137.

- Kafitz, K.W., Guttinger, H.R. and Muller, C.M. "Seasonal changes in astrocytes parallel neuronal plasticity in the song control area of the canary." GLIA 27 (1999): 88-100.
- Marc, R.E., Jones, B.W., Watt, C.B. and Strettoi, E. "Neural remodeling in retinal degeneration." Progress in retinal and eye research 22 (2003): 607-655.
- Medini, P. and Pizzorusso, T. "Visual experience and plasticity of the visual cortex: a role for epigenetic mechanisms." Frontiers in Bioscience 13 (2008): 3000-3008.
- Messing, A. and Brenner, M. "GFAP: Functional implications gleaned from studies of genetically engineered mice." GLIA 43 (2003): 87-90
- Muller, C.M., Akhavan, A.C. and Bette, M. "Possible role of S100 in glia-neuronal signaling involved in activity dependent plasticity in the developing mammalian cortex." Journal of Chemical Neuroanatomy 6 (1993): 215-227
- Piet, R., Vargova, L., Sykova, E., Poulain, D.A. and Oliet, S.H.R. "Physiological contribution of the astrocytic environment of neurons to intersynaptic crosstalk." PNAS 101(7) (2004): 2151-2155.
- Privat, A. "Astrocytes as support for axonal regeneration in the central nervous system of mammals." GLIA 43 (2003): 91-93.
- Rocheftort, N., Quenech' du, N., Watroba, L., Mallat, M., Giaume, C. and Milleret, C. "Microglia and astrocytes may participate in the shaping of visual callosal projections during postnatal development." Journal of Physiology 96 (2002): 183-192.
- Rothermundt, M., Peters, M., Prehn, J.H.M. and Arolt, V. "S100B in brain damage and neurodegeneration." Microscopy Research and Technique 60 (2003):614-632.
- Sambrook and Russell. Molecular Cloning: A Laboratory Manual. New York: Cold Spring Harbor Laboratory Press, 2001.
- Ullian, E.M., Christopherson, K.S. and Barres, B.A. "Role of glia in synaptogenesis." GLIA 47 (2004): 209-216
- Valasek, M.A. and Repa, J.J. "The power of real-time PCR." Advances in Physiology Education 29 (2005): 151-159.
- Yuan, J.S., Reed, A., Chen, F. and Stewart, C.N. Jr. "Statistical analysis of real-time PCR data." BMC Bioinformatics (2006):
- Yuan, J.S., Wang, D. and Stewart, C.N.Jr. "Statistical methods for efficiency adjusted real-time PCR quantification." Biotechnology Journal 3 (2007): 112-123.

# Appendices

## 1) Data for standard and efficiency curve analysis

Treatment	Gene	cDNA	LogBase2 cDNAmean	Ct mean	plustype	interaction	minustype	interaction2
Pde6b -	GAPDH	0.0001	-13.29	33.22	0	0	1	-13.29
Pde6b -	GAPDH	0.001	-9.97	31.07	0	0	1	-9.97
Pde6b -	GAPDH	0.01	-6.64	27.19	0	0	1	-6.64
Pde6b -	GAPDH	0.1	-3.32	23.49	0	0	1	-3.32
Pde6b -	GAPDH	1	0	20.36	0	0	1	0
Pde6b +	GAPDH	0.0001	-13.29	31.66	1	-13.29	0	0
Pde6b +	GAPDH	0.001	-9.97	29.48	1	-9.97	0	0
Pde6b +	GAPDH	0.01	-6.64	25.84	1	-6.64	0	0
Pde6b +	GAPDH	0.1	-3.32	23.53	1	-3.32	0	0
Pde6b +	GAPDH	1	0	19.49	1	0	0	0
Pde6b -	GFAP	0.0001	-13.29	36.29	0	0	1	-13.29
Pde6b -	GFAP	0.001	-9.97	33.02	0	0	1	-9.97
Pde6b -	GFAP	0.01	-6.64	33.08	0	0	1	-6.64
Pde6b -	GFAP	0.1	-3.32	30.84	0	0	1	-3.32
Pde6b -	GFAP	1	0	28.27	0	0	1	0
Pde6b +	GFAP	0.0001	-13.29	35.56	1	-13.29	0	0
Pde6b +	GFAP	0.001	-9.97	31.36	1	-9.97	0	0
Pde6b +	GFAP	0.01	-6.64	29.25	1	-6.64	0	0
Pde6b +	GFAP	0.1	-3.32	29.18	1	-3.32	0	0
Pde6b +	GFAP	1	0	22.46	1	0	0	0
Pde6b -	S100	0.0001	-13.29	36.8	0	0	1	-13.29
Pde6b -	S100	0.001	-9.97	33.21	0	0	1	-9.97
Pde6b -	S100	0.01	-6.64	29.44	0	0	1	-6.64
Pde6b -	S100	0.1	-3.32	26.2	0	0	1	-3.32
Pde6b -	S100	1	0	22.04	0	0	1	0
Pde6b +	S100	0.0001	-13.29	36.53	1	-13.29	0	0
Pde6b +	S100	0.001	-9.97	35.48	1	-9.97	0	0
Pde6b +	S100	0.01	-6.64	32.92	1	-6.64	0	0
Pde6b +	S100	0.1	-3.32	29.16	1	-3.32	0	0
Pde6b +	S100	1	0	22.5	1	0	0	0
Pde6b -	Vimentin	0.0001	-13.29	37.24	0	0	1	-13.29
Pde6b -	Vimentin	0.001	-9.97	35.5	0	0	1	-9.97
Pde6b -	Vimentin	0.01	-6.64	32.89	0	0	1	-6.64
Pde6b -	Vimentin	0.1	-3.32	28.87	0	0	1	-3.32
Pde6b -	Vimentin	1	0	27.01	0	0	1	0
Pde6b +	Vimentin	0.0001	-13.29	35.5	1	-13.29	0	0
Pde6b +	Vimentin	0.001	-9.97	33.56	1	-9.97	0	0
Pde6b +	Vimentin	0.01	-6.64	30.05	1	-6.64	0	0
Pde6b +	Vimentin	0.1	-3.32	26.5	1	-3.32	0	0
Pde6b +	Vimentin	1	0	22	1	0	0	0



## 2) Regression analysis output for standard and efficiency curves

### Regression for Pde6b-

[DataSet1] J:\stats meeting SPSS files 5-28-2008>Data for std and E curve analysis as of 5-27-2008.sav

**Variables Entered/Removed<sup>b</sup>**

Gene	Model	Variables Entered	Variables Removed	Method
GAPDH	1	interaction, Log Base2c DNA_mean, <sup>a</sup> plustype		Enter
GFAP	1	interaction, Log Base2c DNA_mean, <sup>a</sup> plustype		Enter
S100	1	interaction, Log Base2c DNA_mean, <sup>a</sup> plustype		Enter
Vimentin	1	interaction, Log Base2c DNA_mean, <sup>a</sup> plustype		Enter

a. All requested variables entered.

b. Dependent Variable: Ct\_mean

**Model Summary**

Gene	Model	R	R Square	Adjusted R Square	Std. Error of the Estimate
GAPDH	1	.996 <sup>a</sup>	.992	.988	.52966
GFAP	1	.959 <sup>a</sup>	.919	.879	1.39026
S100	1	.979 <sup>a</sup>	.958	.937	1.38076
Vimentin	1	.992 <sup>a</sup>	.984	.976	.75205

a. Predictors: (Constant), interaction, LogBase2cDNA\_mean, plustype

ANOVA<sup>b</sup>

Gene	Model		Sum of Squares	df	Mean Square	F	Sig.
GAPDH	1	Regression	205.421	3	68.474	244.077	.000 <sup>d</sup>
		Residual	1.683	6	.281		
		Total	207.105	9			
GFAP	1	Regression	132.446	3	44.149	22.842	.001 <sup>a</sup>
		Residual	11.597	6	1.933		
		Total	144.043	9			
S100	1	Regression	259.546	3	86.515	45.379	.000 <sup>a</sup>
		Residual	11.439	6	1.906		
		Total	270.985	9			
Vimentin	1	Regression	208.685	3	69.562	122.991	.000 <sup>a</sup>
		Residual	3.394	6	.566		
		Total	212.079	9			

a. Predictors: (Constant), interaction, LogBase2cDNA\_mean, plustype

b. Dependent Variable: Ct\_mean

Coefficients<sup>a</sup>

Gene	Model		Unstandardized Coefficients		Standardized Coefficients	t	Sig.	95% Confidence Interval for B	
			B	Std. Error	Beta			Lower Bound	Upper Bound
GAPDH	1	(Constant)	20.409	.410		49.755	.000	19.405	21.413
		LogBase2cDNA_mean	-1.002	.050	-.1035	-19.876	.000	-1.125	-.878
		plustype	-.467	.580	-.051	-.805	.451	-1.887	.952
		interaction	.090	.071	.093	1.267	.252	-.084	.265
GFAP	1	(Constant)	28.657	1.077		26.616	.000	26.022	31.291
		LogBase2cDNA_mean	-.548	.132	-.679	-4.144	.006	-.872	-.225
		plustype	-4.769	1.523	-.628	-3.132	.020	-8.495	-1.044
		interaction	-.306	.187	-.378	-1.633	.154	-.763	.152
S100	1	(Constant)	22.231	1.069		20.790	.000	19.615	24.848
		LogBase2cDNA_mean	-1.099	.131	-.993	-8.367	.000	-1.421	-.778
		plustype	2.212	1.512	.213	1.463	.194	-1.488	5.913
		interaction	.065	.186	.059	.350	.738	-.390	.520
Vimentin	1	(Constant)	26.884	.582		46.158	.000	25.458	28.309
		LogBase2cDNA_mean	-.815	.072	-.832	-11.393	.000	-.990	-.640
		plustype	-4.171	.824	-.453	-5.064	.002	-6.187	-2.156
		interaction	-.209	.101	-.214	-2.058	.084	-.457	.038

a. Dependent Variable: Ct\_mean

## Regression for Pde6b+

[DataSet1] J: stats meeting SPSS files 5-28-2008 Data for sta and E curve analysis as of 5-27-2008.sav

**Variables Entered/Removed<sup>a</sup>**

Gene	Model	Variables Entered	Variables Removed	Method
GAPDH	1	interaction 2, Log Base2c DNA_mean, minustype <sup>a</sup>		Enter
GFAP	1	interaction 2, Log Base2c DNA_mean, minustype <sup>a</sup>		Enter
S100	1	interaction 2, Log Base2c DNA_mean, minustype <sup>a</sup>		Enter
Vimentin	1	interaction 2, Log Base2c DNA_mean, minustype <sup>a</sup>		Enter

a. All requested variables entered.

b. Dependent Variable: Ct\_mean

**Model Summary**

Gene	Model	R	R Square	Adjusted R Square	Std. Error of the Estimate
GAPDH	1	.996 <sup>a</sup>	.992	.988	.52966
GFAP	1	.959 <sup>a</sup>	.919	.879	1.39026
S100	1	.979 <sup>a</sup>	.958	.937	1.38076
Vimentin	1	.992 <sup>a</sup>	.984	.976	.75205

a. Predictors: (Constant), interaction2, LogBase2cDNA\_mean, minustype

ANOVA<sup>b</sup>

Gene	Model		Sum of Squares	df	Mean Square	F	Sig.
GAPDH	1	Regression	205.421	3	68.474	244.077	.000 <sup>a</sup>
		Residual	1.683	6	.281		
		Total	207.105	9			
GFAP	1	Regression	132.446	3	44.149	22.842	.001 <sup>a</sup>
		Residual	11.597	6	1.933		
		Total	144.043	9			
S100	1	Regression	259.546	3	86.515	45.379	.000 <sup>a</sup>
		Residual	11.439	6	1.906		
		Total	270.985	9			
Vimentin	1	Regression	208.685	3	69.562	122.991	.000 <sup>a</sup>
		Residual	3.394	6	.566		
		Total	212.079	9			

a. Predictors: (Constant), interaction2, LogBase2cDNA\_mean, minustype

b. Dependent Variable: Ct\_mean

Coefficients<sup>a</sup>

Gene	Model		Unstandardized Coefficients		Standardized Coefficients	t	Sig.	95% Confidence Interval for B	
			B	Std. Error	Beta			Lower Bound	Upper Bound
GAPDH	1	(Constant)	19.942	.410		48.616	.000	18.938	20.945
		LogBase2cDNA_mean	-.912	.050	-.941	-18.084	.000	-1.035	-.788
		minustype	.467	.580	.051	.805	.451	-.952	1.887
		interaction2	-.090	.071	-.093	-1.267	.252	-.265	.084
GFAP	1	(Constant)	23.887	1.077		22.186	.000	21.253	26.522
		LogBase2cDNA_mean	-.854	.132	-1.057	-6.454	.001	-1.178	-.530
		minustype	4.769	1.523	.628	3.132	.020	1.044	8.495
		interaction2	.306	.187	.378	1.633	.154	-.152	.763
S100	1	(Constant)	24.444	1.069		22.859	.000	21.827	27.060
		LogBase2cDNA_mean	-1.034	.131	-.934	-7.872	.000	-1.356	-.713
		minustype	-2.212	1.512	-.213	-1.463	.194	-5.913	1.488
		interaction2	-.065	.186	-.059	-.350	.738	-.520	.390
Vimentin	1	(Constant)	22.712	.582		38.996	.000	21.287	24.137
		LogBase2cDNA_mean	-1.025	.072	-1.046	-14.317	.000	-1.200	-.850
		minustype	4.171	.824	.453	5.064	.002	2.156	6.187
		interaction2	.209	.101	.214	2.068	.084	-.038	.457

a. Dependent Variable: Ct\_mean

### 3) Syntax for regression analysis using SPSS

```
SORT CASES BY Gene .  
SPLIT FILE  
  LAYERED BY Gene .
```

```
GRAPH  
  /SCATTERPLOT(BIVAR)=LogBase2cDNA_mean WITH Ct_mean BY Treatment  
  /MISSING=LISTWISE .
```

```
REGRESSION  
  /MISSING LISTWISE  
  /STATISTICS COEFF OUTS CI R ANOVA  
  /CRITERIA=PIN(.05) POUT(.10)  
  /NOORIGIN  
  /DEPENDENT Ct_mean  
  /METHOD=ENTER LogBase2cDNA_mean plustype interaction .
```

```
REGRESSION  
  /MISSING LISTWISE  
  /STATISTICS COEFF OUTS CI R ANOVA  
  /CRITERIA=PIN(.05) POUT(.10)  
  /NOORIGIN  
  /DEPENDENT Ct_mean  
  /METHOD=ENTER LogBase2cDNA_mean minustype interaction2 .
```

#### 4) Data: high and low Ct values for each sample

Genotype	Age	GAPDH		GFAP		S100		Vimentin	
		high	low	high	low	high	low	high	low
WT	PND 7	21.52	21.48	31.15	30.67	31.34	31.23	27.69	26.95
WT	PND 7	20.81	20.61	24.89	24.57	31.9	31.2	26.82	25.89
WT	PND 7	21.37	21.24	26.29	26.21	32.19	31.3	27.41	26.8
RD	PND 7	21.15	21.11	31.91	31.48	31.03	30.57	26.71	26.33
RD	PND 7	23.87	23.14	34.19	34.11	34.09	34.03	30.19	29.68
RD	PND 7	23.16	22.85	35.38	35.19	33.29	33.22	27.84	27.24
WT	PND 14	22.31	21.67	28.55	28.05	27.84	27.24	28	27.56
WT	PND 14	20.81	20.48	27.81	27.13	26.49	26.08	26.13	25.85
WT	PND 14	20.43	20.13	28.44	27.44	26.36	26.33	28.03	27.33
RD	PND 14	20.37	20.01	28.71	28.29	26.49	26.42	27.6	27.5
RD	PND 14	19.99	19.7	27.46	26.46	25.93	25.21	26.11	25.99
RD	PND 14	20.49	20.09	27.03	27.02	26.96	26.75	25.84	25.07
WT	PND 21	21.88	21.72	28.13	27.37	27.54	27.5	27.29	27.25
WT	PND 21	21.27	21.15	27.91	27.79	26.68	26.55	26.58	26.17
WT	PND 21	22.3	21.85	26.64	26.47	27.26	26.9	27.45	27.3
RD	PND 21	21.44	20.73	28.02	27.56	26.89	26.7	27.34	26.81
RD	PND 21	22.9	22.77	27.98	27.84	29.85	29.7	29.87	29.77
RD	PND 21	20.79	20.78	28.89	28.84	26.39	26.35	28.2	27.26
WT	PND 28	20.2	19.99	27.9	27.58	26.51	25.56	26.29	26.18
WT	PND 28	20.63	20.54	27.66	27.24	26.98	26.88	25.26	24.85
WT	PND 28	21.5	21.44	29.47	29.4	27.51	26.74	26.73	25.92
RD	PND 28	24.45	23.54	28.44	28.32	29.96	29.8	28.2	27.79
RD	PND 28	22.95	22.7	31.33	31.15	28.24	27.85	27.95	27.86
RD	PND 28	21.48	21.42	26.34	26.25	27.08	27.02	27.93	27.7
WT	PND 35	21.69	21.32	28.91	28.85	27.63	26.72	27.52	27.28
WT	PND 35	23.33	23.21	29.59	29.42	29.64	28.93	28.3	27.87
WT	PND 35	20.91	20.82	29.08	28.94	26.95	26.73	26.78	26.78
RD	PND 35	20.61	20.17	28.18	27.82	28.96	28.93	30.48	29.74
RD	PND 35	31.24	31.09	35.58	34.64	36.37	36.08	36.02	35.49
RD	PND 35	23.91	22.95	33.41	33.16	30.92	30.15	31.44	31.41
WT	PND 42	21.84	21.79	29.88	29.71	28.09	27.88	28.77	28.74
WT	PND 42	22.32	21.92	29.15	28.63	28.96	28.67	30.61	30.06
WT	PND 42	21.67	21.39	28.41	28.37	27.25	26.92	28.66	27.75
RD	PND 42	22.5	21.88	29.81	29.34	26.5	26.49	29.35	28.63
RD	PND 42	21.77	21.39	28.51	28.47	27.93	27.64	27.79	27.01
RD	PND 42	22.84	21.89	31.29	30.41	27.64	27.52	28.33	27.61
WT	PND 49	20.35	20	27.45	26.62	25.31	25.24	25.82	25.59
WT	PND 49	20.75	20.56	28.57	28.44	26.33	26.23	28.36	27.82
WT	PND 49	23.94	23.66	30.65	29.67	28.89	28.82	31.12	30.31
RD	PND 49	21.99	21.95	30.84	30.65	29.81	28.84	28.26	27.44
RD	PND 49	23.61	23.38	35.43	34.87	30.04	29.39	31.24	30.34
RD	PND 49	21.93	21.8	31.83	30.99	28.61	28	28.23	27.83
WT	PND 100	19.15	19.05	27.79	27.6	25.27	24.3	24.51	24.45
WT	PND 100	23.39	23.35	28.58	28.34	27.33	27.27	31.11	30.12
WT	PND 100	24.95	24.59	32.75	32.23	31.16	30.84	30.3	30.24
RD	PND 100	25.8	25.05	31.57	30.77	28.47	27.74	32.96	32.63
RD	PND 100	20.8	20.65	27.03	26.37	26.96	26.02	28.92	28.07
RD	PND 100	22.24	21.97	32.24	31.3	29.95	29.86	28.91	28.17
WT	PND 140	20.75	20.39	27.96	27.44	26.39	25.85	28.07	27.29
WT	PND 140	21.2	20.71	27.86	27.11	26.81	26.45	25.99	25.56
WT	PND 140	21.65	21.56	28.76	28.44	28.84	28.34	28.17	28.1
WT	PND 140	22.75	21.85	30.52	30.27	27.77	27.5	26.87	26.68
WT	PND 140	20.1	20	30.41	29.59	26.77	26.2	26.36	26.31
RD	PND 140	23.13	23.08	29.29	28.81	28.35	28.32	27.47	27.2
RD	PND 140	22.83	22.34	29.85	29.79	26.96	26.26	28.82	27.83
RD	PND 140	22.93	22.58	31.01	30.75	28.39	28.3	30.81	30.34
RD	PND 140	24.73	24.69	29.2	28.25	28.63	28.52	30.44	30.02
RD	PND 140	24.58	24.38	32.85	32.27	31.91	31.45	31.45	30.58
WT	PND 250	21.4	20.76	30.95	30.34	26.89	26.76	25.87	25.71
WT	PND 250	20.63	20.28	28.54	27.74	26.52	26.3	26.59	26.12
WT	PND 250	19.98	19.98	25.37	25.28	26.72	26.26	27.57	27.42
RD	PND 250	24.85	24.32	30.75	30.22	27.79	27.62	30.42	30.35
RD	PND 250	19.89	19.86	32.62	31.78	26.75	25.78	27.92	27.78
RD	PND 250	22.46	22.39	33.82	33.53	30.93	30.73	28.49	28.18

## 5) Correlation analysis syntax using SPSS

\* We split the file by Age so that SPSS will repeat everything we ask it to do for every level of Age: 7, 14, 21, etc.

```
SORT CASES BY Age .  
SPLIT FILE  
  SEPARATE BY Age .
```

\* We ran bivariate Pearson correlations between the high and low values for each mouse.

```
CORRELATIONS  
/VARIABLES=GAPDHhigh GAPDHlow  
/PRINT=TWOTAIL NOSIG  
/MISSING=PAIRWISE .
```

```
CORRELATIONS  
/VARIABLES= GFAPhigh GFAPlow  
/PRINT=TWOTAIL NOSIG  
/MISSING=PAIRWISE .
```

```
CORRELATIONS  
/VARIABLES=S100high S100low  
/PRINT=TWOTAIL NOSIG  
/MISSING=PAIRWISE .
```

```
CORRELATIONS  
/VARIABLES=VIMENTINhigh VIMENTINlow  
/PRINT=TWOTAIL NOSIG  
/MISSING=PAIRWISE .
```

\* We produced scatterplots and later added the best fit straight lines through Chart Editor (by clicking on the graphs in the output).

```
GRAPH  
/SCATTERPLOT(BIVAR)=GAPDHlow WITH GAPDHhigh  
/MISSING=LISTWISE .
```

```
GRAPH  
/SCATTERPLOT(BIVAR)=GFAPlow WITH GFAPhigh  
/MISSING=LISTWISE .
```

```
GRAPH  
/SCATTERPLOT(BIVAR)=S100low WITH S100high  
/MISSING=LISTWISE .
```

```
GRAPH  
/SCATTERPLOT(BIVAR)=VIMENTINlow WITH VIMENTINhigh  
/MISSING=LISTWISE .
```

## 6) GFAP SPSS correlation statistics

Output Created	06-MAY-2008 13:35:28	
Comments		
Input	Data	F:\Research\GFAP\Current analysis 2-7-08\Latest analysis 041508.2008-05-01 Data Set.sav
	Filter	<none>
	Weight	<none>
	Split File	Age
	N of Rows in Working Data File	64
Missing Value Handling	Definition of Missing	User-defined missing values are treated as missing.
	Cases Used	Statistics for each pair of variables are based on all the cases with valid data for that pair.
Syntax	CORRELATIONS /VARIABLES=GFAPhigh GFAPlow /PRINT=TWOTAIL NOSIG /MISSING=PAIRWISE .	
Resources	Elapsed Time	0:00:00.00

[DataSet1] F:\Research\GFAP\Current analysis 2-7-08\Latest analysis 041508\2008-05-01 Data Set.sav

<b>Age = PND 7</b>		GFAPhigh	GFAPlow
GFAPhigh	Pearson Correlation	1	.999(**)
	Sig. (2-tailed)		.000
	N	6	6
GFAPlow	Pearson Correlation	.999(**)	1
	Sig. (2-tailed)	.000	
	N	6	6

\*\* Correlation is significant at the 0.01 level (2-tailed).

a Age = PND 7

<b>Age = PND 14</b>		GFAPhigh	GFAPlow
GFAPhigh	Pearson Correlation	1	.844(*)
	Sig. (2-tailed)		.035
	N	6	6
GFAPlow	Pearson Correlation	.844(*)	1
	Sig. (2-tailed)	.035	
	N	6	6

\* Correlation is significant at the 0.05 level (2-tailed).

a Age = PND 14

<b>Age = PND 21</b>		GFAPhigh	GFAPlow
GFAPhigh	Pearson Correlation	1	.935(**)
	Sig. (2-tailed)		.006
	N	6	6
GFAPlow	Pearson Correlation	.935(**)	1
	Sig. (2-tailed)	.006	
	N	6	6



\*\* Correlation is significant at the 0.01 level (2-tailed).  
 a Age = PND 21

<b>Age = PND 28</b>		GFAPhigh	GFAPlow
GFAPhigh	Pearson Correlation	1	.997(**)
	Sig. (2-tailed)		.000
	N	6	6
GFAPlow	Pearson Correlation	.997(**)	1
	Sig. (2-tailed)	.000	
	N	6	6

\*\* Correlation is significant at the 0.01 level (2-tailed).  
 a Age = PND 28

<b>Age = PND 35</b>		GFAPhigh	GFAPlow
GFAPhigh	Pearson Correlation	1	.997(**)
	Sig. (2-tailed)		.000
	N	6	6
GFAPlow	Pearson Correlation	.997(**)	1
	Sig. (2-tailed)	.000	
	N	6	6

\*\* Correlation is significant at the 0.01 level (2-tailed).  
 a Age = PND 35

<b>Age = PND 42</b>		GFAPhigh	GFAPlow
GFAPhigh	Pearson Correlation	1	.976(**)
	Sig. (2-tailed)		.001
	N	6	6
GFAPlow	Pearson Correlation	.976(**)	1
	Sig. (2-tailed)	.001	
	N	6	6

\*\* Correlation is significant at the 0.01 level (2-tailed).  
 a Age = PND 42

<b>Age = PND 49</b>		GFAPhigh	GFAPlow
GFAPhigh	Pearson Correlation	1	.992(**)
	Sig. (2-tailed)		.000
	N	6	6
GFAPlow	Pearson Correlation	.992(**)	1
	Sig. (2-tailed)	.000	
	N	6	6

\*\* Correlation is significant at the 0.01 level (2-tailed).  
 a Age = PND 49

<b>Age = PND 100</b>		GFAPhigh	GFAPlow
GFAPhigh	Pearson Correlation	1	.994(**)
	Sig. (2-tailed)		.000
	N	6	6
GFAPlow	Pearson Correlation	.994(**)	1
	Sig. (2-tailed)	.000	
	N	6	6

\*\* Correlation is significant at the 0.01 level (2-tailed).  
a Age = PND 100

<b>Age = PND 140</b>		GFAPhigh	GFAPlow
GFAPhigh	Pearson Correlation	1	.984(**)
	Sig. (2-tailed)		.000
	N	10	10
GFAPlow	Pearson Correlation	.984(**)	1
	Sig. (2-tailed)	.000	
	N	10	10

\*\* Correlation is significant at the 0.01 level (2-tailed).  
a Age = PND 140

<b>Age = PND 250</b>		GFAPhigh	GFAPlow
GFAPhigh	Pearson Correlation	1	.996(**)
	Sig. (2-tailed)		.000
	N	6	6
GFAPlow	Pearson Correlation	.996(**)	1
	Sig. (2-tailed)	.000	
	N	6	6

\*\* Correlation is significant at the 0.01 level (2-tailed).  
a Age = PND 250

## 7) Vimentin SPSS correlation statistics

Output Created		06-MAY-2008 13:36:52
Comments		
Input	Data	F:\Research\GFAP\Current analysis 2-7-08\Latest analysis 041508\2008-05-01 Data Set.sav
	Filter	<none>
	Weight	<none>
	Split File	Age
	N of Rows in Working Data File	64
Missing Value Handling	Definition of Missing	User-defined missing values are treated as missing.
	Cases Used	Statistics for each pair of variables are based on all the cases with valid data for that pair.
Syntax		CORRELATIONS /VARIABLES=Vimentinhigh Vimentinlow /PRINT=TWOTAIL NOSIG /MISSING=PAIRWISE .
Resources	Elapsed Time	0:00:00.00

[DataSet1] F:\Research\GFAP\Current analysis 2-7-08\Latest analysis 041508\2008-05-01 Data Set.sav

<b>Age = PND 7</b>		VIMENTINhigh	VIMENTINlow
VIMENTINhigh	Pearson Correlation	1	.990(**)
	Sig. (2-tailed)		.000
	N	6	6
VIMENTINlow	Pearson Correlation	.990(**)	1
	Sig. (2-tailed)	.000	
	N	6	6

\*\* Correlation is significant at the 0.01 level (2-tailed).

a Age = PND 7

<b>Age = PND 14</b>		VIMENTINhigh	VIMENTINlow
VIMENTINhigh	Pearson Correlation	1	.962(**)
	Sig. (2-tailed)		.002
	N	6	6
VIMENTINlow	Pearson Correlation	.962(**)	1
	Sig. (2-tailed)	.002	
	N	6	6

\*\* Correlation is significant at the 0.01 level (2-tailed).

a Age = PND 14

<b>Age = PND 21</b>		VIMENTINhigh	VIMENTINlow
VIMENTINhigh	Pearson Correlation	1	.961(**)
	Sig. (2-tailed)		.002
	N	6	6
VIMENTINlow	Pearson Correlation	.961(**)	1
	Sig. (2-tailed)	.002	
	N	6	6

\*\* Correlation is significant at the 0.01 level (2-tailed).

a Age = PND 21

<b>Age = PND 28</b>		VIMENTINhigh	VIMENTINlow
VIMENTINhigh	Pearson Correlation	1	.978(**)
	Sig. (2-tailed)		.001
	N	6	6
VIMENTINlow	Pearson Correlation	.978(**)	1
	Sig. (2-tailed)	.001	
	N	6	6

\*\* Correlation is significant at the 0.01 level (2-tailed).

a Age = PND 28

<b>Age = PND 35</b>		VIMENTIN high	VIMENTINlow
VIMENTINhigh	Pearson Correlation	1	.997(**)
	Sig. (2-tailed)		.000
	N	6	6
VIMENTINlow	Pearson Correlation	.997(**)	1
	Sig. (2-tailed)	.000	
	N	6	6

\*\* Correlation is significant at the 0.01 level (2-tailed).

a Age = PND 35

<b>Age = PND 42</b>		VIMENTIN high	VIMENTINlow
VIMENTINhigh	Pearson Correlation	1	.960(**)
	Sig. (2-tailed)		.002
	N	6	6
VIMENTINlow	Pearson Correlation	.960(**)	1
	Sig. (2-tailed)	.002	
	N	6	6

\*\* Correlation is significant at the 0.01 level (2-tailed).

a Age = PND 42

<b>Age = PND 49</b>		VIMENTIN high	VIMENTINlow
VIMENTINhigh	Pearson Correlation	1	.997(**)
	Sig. (2-tailed)		.000
	N	6	6
VIMENTINlow	Pearson Correlation	.997(**)	1
	Sig. (2-tailed)	.000	
	N	6	6

\*\* Correlation is significant at the 0.01 level (2-tailed).

a Age = PND 49

<b>Age = PND 100</b>		VIMENTIN high	VIMENTINlow
VIMENTINhigh	Pearson Correlation	1	.990(**)
	Sig. (2-tailed)		.000
	N	6	6
VIMENTINlow	Pearson Correlation	.990(**)	1
	Sig. (2-tailed)	.000	
	N	6	6

\*\* Correlation is significant at the 0.01 level (2-tailed).

a Age = PND 100

<b>Age = PND 140</b>		VIMENTIN	
		high	VIMENTINlow
VIMENTINhigh	Pearson Correlation	1	.987(**)
	Sig. (2-tailed)		.000
	N	10	10
VIMENTINlow	Pearson Correlation	.987(**)	1
	Sig. (2-tailed)	.000	
	N	10	10

\*\* Correlation is significant at the 0.01 level (2-tailed).  
a Age = PND 140

<b>Age = PND 250</b>		VIMENTIN	
		high	VIMENTINlow
VIMENTINhigh	Pearson Correlation	1	.997(**)
	Sig. (2-tailed)		.000
	N	6	6
VIMENTINlow	Pearson Correlation	.997(**)	1
	Sig. (2-tailed)	.000	
	N	6	6

\*\* Correlation is significant at the 0.01 level (2-tailed).  
a Age = PND 250

### 8) S100 SPSS correlation statistics

Output Created		06-MAY-2008 13:33:53
Comments		
Input	Data	F:\Research\GFAP\Current analysis 2-7-08\Latest analysis 041508\2008-05-01 Data Set.sav
	Filter	<none>
	Weight	<none>
	Split File	Age
	N of Rows in Working Data File	64
Missing Value Handling	Definition of Missing	User-defined missing values are treated as missing.
	Cases Used	Statistics for each pair of variables are based on all the cases with valid data for that pair.
Syntax		CORRELATIONS /VARIABLES=S100high S100low /PRINT=TWOTAIL NOSIG /MISSING=PAIRWISE .
Resources	Elapsed Time	0:00:00.09

[DataSet1] F:\Research\GFAP\Current analysis 2-7-08\Latest analysis 041508\2008-05-01 Data Set.sav

<b>Age = PND 7</b>		S100high	S100low
S100high	Pearson Correlation	1	.972(**)
	Sig. (2-tailed)		.001
	N	6	6
S100low	Pearson Correlation	.972(**)	1
	Sig. (2-tailed)	.001	
	N	6	6

\*\* Correlation is significant at the 0.01 level (2-tailed).  
 a Age = PND 7

<b>Age = PND 14</b>		S100high	S100low
S100high	Pearson Correlation	1	.911(*)
	Sig. (2-tailed)		.012
	N	6	6
S100low	Pearson Correlation	.911(*)	1
	Sig. (2-tailed)	.012	
	N	6	6

\* Correlation is significant at the 0.05 level (2-tailed).  
 a Age = PND 14

<b>Age = PND 21</b>		S100high	S100low
S100high	Pearson Correlation	1	.996(**)
	Sig. (2-tailed)		.000
	N	6	6
S100low	Pearson Correlation	.996(**)	1
	Sig. (2-tailed)	.000	
	N	6	6

\*\* Correlation is significant at the 0.01 level (2-tailed).  
 a Age = PND 21

<b>Age = PND 28</b>		S100high	S100low
S100high	Pearson Correlation	1	.969(**)
	Sig. (2-tailed)		.001
	N	6	6
S100low	Pearson Correlation	.969(**)	1
	Sig. (2-tailed)	.001	
	N	6	6

\*\* Correlation is significant at the 0.01 level (2-tailed).  
 a Age = PND 28

<b>Age = PND 35</b>		S100high	S100low
S100high	Pearson Correlation	1	.995(**)
	Sig. (2-tailed)		.000
	N	6	6
S100low	Pearson Correlation	.995(**)	1
	Sig. (2-tailed)	.000	
	N	6	6

\*\* Correlation is significant at the 0.01 level (2-tailed).  
 a Age = PND 35

<b>Age = PND 42</b>		S100high	S100low
S100high	Pearson Correlation	1	.992(**)
	Sig. (2-tailed)		.000
	N	6	6
S100low	Pearson Correlation	.992(**)	1
	Sig. (2-tailed)	.000	
	N	6	6

\*\* Correlation is significant at the 0.01 level (2-tailed).

a Age = PND 42

<b>Age = PND 49</b>		S100high	S100low
S100high	Pearson Correlation	1	.988(**)
	Sig. (2-tailed)		.000
	N	6	6
S100low	Pearson Correlation	.988(**)	1
	Sig. (2-tailed)	.000	
	N	6	6

\*\* Correlation is significant at the 0.01 level (2-tailed).

a Age = PND 49

<b>Age = PND 100</b>		S100high	S100low
S100high	Pearson Correlation	1	.991(**)
	Sig. (2-tailed)		.000
	N	6	6
S100low	Pearson Correlation	.991(**)	1
	Sig. (2-tailed)	.000	
	N	6	6

\*\* Correlation is significant at the 0.01 level (2-tailed).

a Age = PND 100

<b>Age = PND 140</b>		S100high	S100low
S100high	Pearson Correlation	1	.991(**)
	Sig. (2-tailed)		.000
	N	10	10
S100low	Pearson Correlation	.991(**)	1
	Sig. (2-tailed)	.000	
	N	10	10

\*\* Correlation is significant at the 0.01 level (2-tailed).

a Age = PND 140

<b>Age = PND 250</b>		S100high	S100low
S100high	Pearson Correlation	1	.986(**)
	Sig. (2-tailed)		.000
	N	6	6
S100low	Pearson Correlation	.986(**)	1
	Sig. (2-tailed)	.000	
	N	6	6

\*\* Correlation is significant at the 0.01 level (2-tailed).

a Age = PND 250

### 9) GAPDH SPSS correlation statistics

Output Created	06-MAY-2008 13:36:09		
Comments			
Input	Data	F:\Research\GFAP\Current analysis 2-7-08\Latest analysis 041508\2008-05-01 Data Set.sav	
	Filter	<none>	
	Weight	<none>	
	Split File	Age	
	N of Rows in Working Data File	64	
Missing Value Handling	Definition of Missing	User-defined missing values are treated as missing.	
	Cases Used	Statistics for each pair of variables are based on all the cases with valid data for that pair.	
Syntax	CORRELATIONS /VARIABLES=GAPDHhigh GAPDHlow /PRINT=TWOTAIL NOSIG /MISSING=PAIRWISE .		
Resources	Elapsed Time	0:00:00.00	

[DataSet1] F:\Research\GFAP\Current analysis 2-7-08\Latest analysis 041508\2008-05-01 Data Set.sav

<b>Age = PND 7</b>		GAPDHhigh	GAPDHlow
GAPDHhigh	Pearson Correlation	1	.991(**)
	Sig. (2-tailed)		.000
	N	6	6
GAPDHlow	Pearson Correlation	.991(**)	1
	Sig. (2-tailed)	.000	
	N	6	6

\*\* Correlation is significant at the 0.01 level (2-tailed).

a Age = PND 7

<b>Age = PND 14</b>		GAPDHhigh	GAPDHlow
GAPDHhigh	Pearson Correlation	1	.998(**)
	Sig. (2-tailed)		.000
	N	6	6
GAPDHlow	Pearson Correlation	.998(**)	1
	Sig. (2-tailed)	.000	
	N	6	6

\*\* Correlation is significant at the 0.01 level (2-tailed).

a Age = PND 14



<b>Age = PND 21</b>		GAPDHhigh	GAPDHlow
GAPDHhigh	Pearson Correlation	1	.941(**)
	Sig. (2-tailed)		.005
	N	6	6
GAPDHlow	Pearson Correlation	.941(**)	1
	Sig. (2-tailed)	.005	
	N	6	6

\*\* Correlation is significant at the 0.01 level (2-tailed).

a Age = PND 21

<b>Age = PND 28</b>		GAPDHhigh	GAPDHlow
GAPDHhigh	Pearson Correlation	1	.990(**)
	Sig. (2-tailed)		.000
	N	6	6
GAPDHlow	Pearson Correlation	.990(**)	1
	Sig. (2-tailed)	.000	
	N	6	6

\*\* Correlation is significant at the 0.01 level (2-tailed).

a Age = PND 28

<b>Age = PND 35</b>		GAPDHhigh	GAPDHlow
GAPDHhigh	Pearson Correlation	1	.997(**)
	Sig. (2-tailed)		.000
	N	6	6
GAPDHlow	Pearson Correlation	.997(**)	1
	Sig. (2-tailed)	.000	
	N	6	6

\*\* Correlation is significant at the 0.01 level (2-tailed).

a Age = PND 35

<b>Age = PND 42</b>		GAPDHhigh	GAPDHlow
GAPDHhigh	Pearson Correlation	1	.797
	Sig. (2-tailed)		.058
	N	6	6
GAPDHlow	Pearson Correlation	.797	1
	Sig. (2-tailed)	.058	
	N	6	6

a Age = PND 42

<b>Age = PND 49</b>		GAPDHhigh	GAPDHlow
GAPDHhigh	Pearson Correlation	1	.997(**)
	Sig. (2-tailed)		.000
	N	6	6
GAPDHlow	Pearson Correlation	.997(**)	1
	Sig. (2-tailed)	.000	
	N	6	6

\*\* Correlation is significant at the 0.01 level (2-tailed).

a Age = PND 49

<b>Age = PND 100</b>		GAPDHhigh	GAPDHlow
GAPDHhigh	Pearson Correlation	1	.997(**)
	Sig. (2-tailed)		.000
	N	6	6
GAPDHlow	Pearson Correlation	.997(**)	1
	Sig. (2-tailed)	.000	
	N	6	6

\*\* Correlation is significant at the 0.01 level (2-tailed).

a Age = PND 100

<b>Age = PND 140</b>		GAPDHhigh	GAPDHlow
GAPDHhigh	Pearson Correlation	1	.986(**)
	Sig. (2-tailed)		.000
	N	10	10
GAPDHlow	Pearson Correlation	.986(**)	1
	Sig. (2-tailed)	.000	
	N	10	10

\*\* Correlation is significant at the 0.01 level (2-tailed).

a Age = PND 140

<b>Age = PND 250</b>		GAPDHhigh	GAPDHlow
GAPDHhigh	Pearson Correlation	1	.991(**)
	Sig. (2-tailed)		.000
	N	6	6
GAPDHlow	Pearson Correlation	.991(**)	1
	Sig. (2-tailed)	.000	
	N	6	6

\*\* Correlation is significant at the 0.01 level (2-tailed).

a Age = PND 250

## 10) Data: ACt values

Animal Genotype	Age	ACt GF-AP	ACt S100	ACt Vimentin
Wild type	PND 7	9.41	9.79	5.82
Wild type	PND 7	4.02	10.84	5.65
Wild type	PND 7	4.94	10.44	5.8
Retinal degeneration	PND 7	10.57	9.67	5.39
Retinal degeneration	PND 7	10.64	10.55	6.43
Retinal degeneration	PND 7	12.28	10.25	4.53
Wild type	PND 14	6.31	5.55	5.79
Wild type	PND 14	6.82	5.64	5.34
Wild type	PND 14	7.66	6.07	7.4
Retinal degeneration	PND 14	8.31	6.27	7.36
Retinal degeneration	PND 14	7.11	5.72	6.2
Retinal degeneration	PND 14	6.74	6.57	5.17
Wild type	PND 21	5.95	5.72	5.47
Wild type	PND 21	6.64	5.41	5.17
Wild type	PND 21	4.48	5	5.3
Retinal degeneration	PND 21	6.7	5.71	5.99
Retinal degeneration	PND 21	5.07	6.94	6.98
Retinal degeneration	PND 21	8.08	5.58	6.94
Wild type	PND 28	7.64	5.94	6.14
Wild type	PND 28	6.86	6.34	4.47
Wild type	PND 28	7.97	5.66	4.86
Retinal degeneration	PND 28	4.38	5.88	4
Retinal degeneration	PND 28	8.41	5.22	5.08
Retinal degeneration	PND 28	4.85	5.6	6.37
Wild type	PND 35	7.37	5.67	5.89
Wild type	PND 35	6.24	6.02	4.82
Wild type	PND 35	8.14	5.97	5.91
Retinal degeneration	PND 35	7.61	8.56	9.72
Retinal degeneration	PND 35	3.94	5.06	4.59
Retinal degeneration	PND 35	9.86	7.11	8
Wild type	PND 42	7.98	6.17	6.94
Wild type	PND 42	6.77	6.7	8.22
Wild type	PND 42	6.86	5.56	6.68
Retinal degeneration	PND 42	7.39	4.31	6.8
Retinal degeneration	PND 42	6.91	6.21	5.82
Retinal degeneration	PND 42	8.48	5.21	5.6
Wild type	PND 49	6.87	5.11	5.54
Wild type	PND 49	7.85	5.62	7.43
Wild type	PND 49	6.36	5.06	6.92
Retinal degeneration	PND 49	8.78	7.36	5.88
Retinal degeneration	PND 49	11.65	6.22	7.29
Retinal degeneration	PND 49	9.54	6.44	6.16
Wild type	PND 100	8.6	5.69	5.38
Wild type	PND 100	5.09	3.93	7.25
Wild type	PND 100	7.72	6.23	5.5
Retinal degeneration	PND 100	5.74	2.68	7.37
Retinal degeneration	PND 100	5.97	5.76	7.77
Retinal degeneration	PND 100	9.66	7.8	6.43
Wild type	PND 140	7.13	5.55	7.11
Wild type	PND 140	6.53	5.67	4.82
Wild type	PND 140	6.99	6.98	6.53
Wild type	PND 140	8.1	5.34	4.48
Wild type	PND 140	9.95	6.44	6.29
Retinal degeneration	PND 140	5.94	5.23	4.23
Retinal degeneration	PND 140	7.23	4.02	5.74
Retinal degeneration	PND 140	8.12	5.59	7.82
Retinal degeneration	PND 140	4.02	3.87	5.52
Retinal degeneration	PND 140	8.08	7.2	6.54
Wild type	PND 250	9.57	5.75	4.71
Wild type	PND 250	7.68	5.95	5.9
Wild type	PND 250	5.35	6.51	7.52
Retinal degeneration	PND 250	5.9	3.12	5.8
Retinal degeneration	PND 250	12.32	6.39	7.97
Retinal degeneration	PND 250	11.25	8.4	5.91

## 11) ACT t-test analysis syntax using SPSS

\*We run the analysis separately for each time point. Start by splitting the file by Age again.  
 SORT CASES BY Age .  
 SPLIT FILE  
 SEPARATE BY Age .

### T-TEST

```
GROUPS = Genotype(1 2)
/MISSING = ANALYSIS
/VARIABLES = GFAPvCT S100vCT VIMENTINvCT
/CRITERIA = CI(.95) .
```

## 12) T-test output each gene/age using SPSS

### T-Test

[DataSet1] C:\Documents and Settings\arieck\Local Settings\Temporary Internet Files\Content.IE5\Q5U5I1K3\2008-05-01%20Data%20Set [1].sav  
 Age = PND 7

Group Statistics<sup>a</sup>

Genotype		N	Mean	Std. Deviation	Std. Error Mean
GFAPvCT	Wild type	3	6.1233	2.88327	1.66466
	Retinal degeneration	3	11.1633	.96769	.55870
S100vCT	Wild type	3	10.3567	.52994	.30596
	Retinal degeneration	3	10.1567	.44736	.25828
VIMENTINvCT	Wild type	3	5.7567	.09292	.05364
	Retinal degeneration	3	5.4500	.95142	.54930

a. Age = PND 7

Independent Samples Test

		Levene's Test for Equality of Variances		t-test for Equality of Means						
		F	Sig.	t	df	Sig. (2-tailed)	Mean Difference	Std. Error Difference	95% Confidence Interval of the Difference	
									Lower	Upper
GFAPvCT	Equal variances assumed	5.159	.086	-2.870	4	.045	-5.04000	1.75591	-9.91519	-.16481
	Equal variances not assumed			-2.870	2.445	.082	-5.04000	1.75591	-11.41909	1.33909
S100vCT	Equal variances assumed	.078	.794	.499	4	.644	.20000	.40040	-.91170	1.31170
	Equal variances not assumed			.499	3.890	.644	.20000	.40040	-.92415	1.32415
VIMENTINvCT	Equal variances assumed	3.823	.122	.556	4	.608	.30667	.55192	-1.22570	1.83903
	Equal variances not assumed			.556	2.038	.633	.30667	.55192	-2.02595	2.63928

a. Age = PND 7

Age = PND 14

Group Statistics<sup>a</sup>

Genotype		N	Mean	Std. Deviation	Std. Error Mean
GFAPvCT	Wild type	3	6.9300	.68169	.39357
	Retinal degeneration	3	7.3867	.82075	.47386
S100vCT	Wild type	3	5.7533	.27791	.16045
	Retinal degeneration	3	6.1867	.43108	.24889
VIMENTINvCT	Wild type	3	6.1767	1.08307	.62531
	Retinal degeneration	3	6.2433	1.09564	.63257

a. Age = PND 14

Independent Samples Test

		Levene's Test for Equality of Variances		t-test for Equality of Means						
		F	Sig.	t	df	Sig. (2-tailed)	Mean Difference	Std. Error Difference	95% Confidence Interval of the Difference	
									Lower	Upper
GFAPvCT	Equal variances assumed	.232	.655	-.741	4	.500	-.45667	.61599	-2.16693	1.25360
	Equal variances not assumed			-.741	3.870	.501	-.45667	.61599	-2.18989	1.27656
S100vCT	Equal variances assumed	.588	.486	-1.463	4	.217	-.43333	.29612	-1.25550	.38884
	Equal variances not assumed			-1.463	3.418	.229	-.43333	.29612	-1.31382	.44716
VIMENTINvCT	Equal variances assumed	.028	.876	-.075	4	.944	-.06667	.88947	-2.53623	2.40200
	Equal variances not assumed			-.075	3.999	.944	-.06667	.88947	-2.53636	2.40303

a. Age = PND 14

Age = PND 21

Group Statistics<sup>a</sup>

Genotype		N	Mean	Std. Deviation	Std. Error Mean
GFAPvCT	Wild type	3	5.6900	1.10322	.63695
	Retinal degeneration	3	6.6167	1.50673	.86991
S100vCT	Wild type	3	5.3767	.36116	.20851
	Retinal degeneration	3	6.0767	.75049	.43329
VIMENTINvCT	Wild type	3	5.3133	.15044	.08686
	Retinal degeneration	3	6.6367	.56039	.32354

a. Age = PND 21

Independent Samples Test

		Levene's Test for Equality of Variances		t-test for Equality of Means						
		F	Sig.	t	df	Sig. (2-tailed)	Mean Difference	Std. Error Difference	95% Confidence Interval of the Difference	
									Lower	Upper
GFAPvCT	Equal variances assumed	.165	.705	-.859	4	.439	-.92667	1.07817	-3.92014	2.06681
	Equal variances not assumed			-.859	3.666	.443	-.92667	1.07817	-4.03094	2.17760
S100vCT	Equal variances assumed	3.090	.154	-1.456	4	.219	-.70000	.48086	-2.03507	.63507
	Equal variances not assumed			-1.456	2.879	.245	-.70000	.48086	-2.26728	.86728
VIMENTINvCT	Equal variances assumed	7.711	.050	-3.950	4	.017	-1.32333	.33500	-2.25343	-.39324
	Equal variances not assumed			-3.950	2.287	.047	-1.32333	.33500	-2.60461	-.04206

a. Age = PND 21

Age = PND 28

Group Statistics<sup>a</sup>

Genotype		N	Mean	Std. Deviation	Std. Error Mean
GFAPvCT	Wild type	3	7.4900	.57000	.32909
	Retinal degeneration	3	5.8800	2.20361	1.27226
S100vCT	Wild type	3	5.9800	.34176	.19732
	Retinal degeneration	3	5.5667	.33126	.19125
VIMENTINvCT	Wild type	3	5.1567	.87363	.50439
	Retinal degeneration	3	5.1500	1.18655	.68505

a. Age = PND 28

Independent Samples Test

		Levene's Test for Equality of Variances		t-test for Equality of Means						
		F	Sig.	t	df	Sig. (2-tailed)	Mean Difference	Std. Error Difference	95% Confidence Interval of the Difference	
									Lower	Upper
GFAPvCT	Equal variances assumed	7.417	.053	1.225	4	.288	1.61000	1.31413	-2.03861	5.25861
	Equal variances not assumed			1.225	2.266	.333	1.61000	1.31413	-3.45268	6.67268
S100vCT	Equal variances assumed	.004	.953	1.504	4	.207	.41333	.27479	-.34961	1.17628
	Equal variances not assumed			1.504	3.996	.207	.41333	.27479	-.34991	1.17657
VIMENTINvCT	Equal variances assumed	.140	.727	.008	4	.994	.00667	.85071	-2.35529	2.36862
	Equal variances not assumed			.008	3.676	.994	.00667	.85071	-2.43973	2.45306

a. Age = PND 28

Age = PND 35

**Group Statistics<sup>a</sup>**

Genotype		N	Mean	Std. Deviation	Std. Error Mean
GFAPvCT	Wild type	3	7.2500	.95567	.55175
	Retinal degeneration	3	7.1367	2.98825	1.72527
S100vCT	Wild type	3	5.8867	.18930	.10929
	Retinal degeneration	3	6.9100	1.75855	1.01530
VIMENTINvCT	Wild type	3	5.5400	.62362	.36005
	Retinal degeneration	3	7.4367	2.61098	1.50745

a. Age = PND 35

**Independent Samples Test**

		Levene's Test for Equality of Variances		t-test for Equality of Means						
		F	Sig.	t	df	Sig. (2-tailed)	Mean Difference	Std. Error Difference	95% Confidence Interval of the Difference	
									Lower	Upper
GFAPvCT	Equal variances assumed	2.712	.175	.063	4	.953	.11333	1.81135	-4.91577	5.14244
	Equal variances not assumed			.063	2.405	.955	.11333	1.81135	-6.54858	6.77524
S100vCT	Equal variances assumed	4.362	.105	-1.002	4	.373	-1.02333	1.02116	-3.85854	1.81187
	Equal variances not assumed			-1.002	2.046	.420	-1.02333	1.02116	-5.32306	3.27640
VIMENTINvCT	Equal variances assumed	4.135	.112	-1.224	4	.288	-1.89667	1.54985	-6.19975	2.40642
	Equal variances not assumed			-1.224	2.227	.335	-1.89667	1.54985	-7.95330	4.15997

a. Age = PND 35

**Age = PND 42**

**Group Statistics<sup>a</sup>**

Genotype		N	Mean	Std. Deviation	Std. Error Mean
GFAPvCT	Wild type	3	7.2033	.67412	.38920
	Retinal degeneration	3	7.5933	.80451	.46448
S100vCT	Wild type	3	6.1433	.57047	.32936
	Retinal degeneration	3	5.2433	.95044	.54874
VIMENTINvCT	Wild type	3	7.2800	.82438	.47596
	Retinal degeneration	3	6.0733	.63885	.36884

a. Age = PND 42

Independent Samples Test<sup>a</sup>

		Levene's Test for Equality of Variances		t-test for Equality of Means					95% Confidence Interval of the Difference	
		F	Sig.	t	df	Sig. (2-tailed)	Mean Difference	Std. Error Difference	Lower	Upper
GFAPvCT	Equal variances assumed	.092	.777	-.644	4	.555	-.39000	.60599	-2.07249	1.29249
	Equal variances not assumed			-.644	3.881	.556	-.39000	.60599	-2.09301	1.31301
S100vCT	Equal variances assumed	.517	.512	1.406	4	.232	.90000	.63999	-.87690	2.67690
	Equal variances not assumed			1.406	3.275	.247	.90000	.63999	-1.04318	2.84318
VIMENTINvCT	Equal variances assumed	.414	.555	2.004	4	.116	1.20667	.60214	-.46515	2.87849
	Equal variances not assumed			2.004	3.765	.120	1.20667	.60214	-.50703	2.92037

a. Age = PND 42

Age = PND 49

Group Statistics<sup>a</sup>

Genotype		N	Mean	Std. Deviation	Std. Error Mean
GFAPvCT	Wild type	3	7.0267	.75725	.43720
	Retinal degeneration	3	9.9900	1.48698	.85851
S100vCT	Wild type	3	5.2633	.30989	.17892
	Retinal degeneration	3	6.6733	.60476	.34916
VIMENTINvCT	Wild type	3	6.6300	.97780	.56454
	Retinal degeneration	3	6.4433	.74648	.43098

a. Age = PND 49

Independent Samples Test

		Levene's Test for Equality of Variances		t-test for Equality of Means					95% Confidence Interval of the Difference	
		F	Sig.	t	df	Sig. (2-tailed)	Mean Difference	Std. Error Difference	Lower	Upper
GFAPvCT	Equal variances assumed	1.883	.242	-3.076	4	.037	-2.96333	.96342	-5.63822	-.28845
	Equal variances not assumed			-3.076	2.972	.055	-2.96333	.96342	-6.04577	.11911
S100vCT	Equal variances assumed	2.319	.202	-3.594	4	.023	-1.41000	.39233	-2.49928	-.32072
	Equal variances not assumed			-3.594	2.983	.037	-1.41000	.39233	-2.66271	-.15729
VIMENTINvCT	Equal variances assumed	.324	.599	.263	4	.806	.18667	.71024	-1.78528	2.15862
	Equal variances not assumed			.263	3.740	.807	.18667	.71024	-1.84050	2.21383

a. Age = PND 49

Age = PND 100



**Group Statistics<sup>a</sup>**

Genotype		N	Mean	Std. Deviation	Std. Error Mean
GFAPvCT	Wild type	3	7.1367	1.82626	1.05439
	Retinal degeneration	3	7.1233	2.19983	1.27007
S100vCT	Wild type	3	5.2833	1.20272	.69439
	Retinal degeneration	3	5.4133	2.57754	1.48815
VIMENTINvCT	Wild type	3	6.0433	1.04673	.60433
	Retinal degeneration	3	7.1900	.68790	.39716

a. Age = PND 100

**Independent Samples Test**

		Levene's Test for Equality of Variances		t-test for Equality of Means					95% Confidence Interval of the Difference	
		F	Sig.	t	df	Sig. (2-tailed)	Mean Difference	Std. Error Difference	Lower	Upper
									Equal variances assumed	Equal variances not assumed
GFAPvCT	Equal variances assumed	293	.617	.008	4	.994	.01333	1.65070	-4.56975	4.59642
	Equal variances not assumed			.008	3.869	.994	.01333	1.65070	-4.63159	4.65826
S100vCT	Equal variances assumed	1.345	.311	-.079	4	.941	-.13000	1.64218	-4.68942	4.42942
	Equal variances not assumed			-.079	2.831	.942	-.13000	1.64218	-5.53658	5.27658
VIMENTINvCT	Equal variances assumed	1.248	.326	-1.586	4	.188	-1.14667	.72315	-3.15145	.86112
	Equal variances not assumed			-1.586	3.456	.199	-1.14667	.72315	-3.28545	.99212

a. Age = PND 100

**Age = PND 140**

**Group Statistics<sup>a</sup>**

Genotype		N	Mean	Std. Deviation	Std. Error Mean
GFAPvCT	Wild type	5	7.7400	1.36129	.60879
	Retinal degeneration	5	6.6780	1.72911	.77328
S100vCT	Wild type	5	5.9960	.68937	.30830
	Retinal degeneration	5	5.1820	1.35210	.60468
VIMENTINvCT	Wild type	5	5.8460	1.13813	.50899
	Retinal degeneration	5	5.9700	1.32575	.59289

a. Age = PND 140

Independent Samples Test<sup>a</sup>

		Levene's Test for Equality of Variances		t-test for Equality of Means					95% Confidence Interval of the Difference	
		F	Sig.	t	df	Sig. (2-tailed)	Mean Difference	Std. Error Difference	Lower	Upper
GFAPvCT	Equal variances assumed	.449	.522	1.079	8	.312	1.06200	.98417	-1.20749	3.33149
	Equal variances not assumed			1.079	7.582	.314	1.06200	.98417	-1.22944	3.35344
S100vCT	Equal variances assumed	1.304	.287	1.199	8	.265	.81400	.67873	-.75116	2.37916
	Equal variances not assumed			1.199	5.948	.276	.81400	.67873	-.85033	2.47833
VIMENTINvCT	Equal variances assumed	.001	.977	-1.159	8	.878	-.12400	.78140	-1.92591	1.67791
	Equal variances not assumed			-1.159	7.821	.878	-.12400	.78140	-1.93313	1.68513

a. Age = PND 140

Age = PND 250

Group Statistics<sup>a</sup>

Genotype		N	Mean	Std. Deviation	Std. Error Mean
GFAPvCT	Wild type	3	7.5333	2.11382	1.22041
	Retinal degeneration	3	9.8233	3.43957	1.98584
S100vCT	Wild type	3	6.0700	.39395	.22745
	Retinal degeneration	3	5.9700	2.66494	1.53860
VIMENTINvCT	Wild type	3	6.0433	1.41047	.81434
	Retinal degeneration	3	6.5600	1.22233	.70571

a. Age = PND 250

Independent Samples Test

		Levene's Test for Equality of Variances		t-test for Equality of Means					95% Confidence Interval of the Difference	
		F	Sig.	t	df	Sig. (2-tailed)	Mean Difference	Std. Error Difference	Lower	Upper
GFAPvCT	Equal variances assumed	1.412	.300	-1.982	4	.381	-2.29000	2.33087	-8.76153	4.18153
	Equal variances not assumed			-1.982	3.322	.392	-2.29000	2.33087	-9.31710	4.73710
S100vCT	Equal variances assumed	4.521	.101	.064	4	.952	.10000	1.55532	-4.21827	4.41827
	Equal variances not assumed			.064	2.087	.954	.10000	1.55532	-6.33063	6.53063
VIMENTINvCT	Equal variances assumed	.008	.931	-.479	4	.657	-.51667	1.07758	-3.50851	2.47517
	Equal variances not assumed			-.479	3.921	.657	-.51667	1.07758	-3.53252	2.49918

a. Age = PND 250

### 13) Graphing $\Delta$ Ct for each gene syntax using SPSS

\* Here we turn off the splitting of the file.

```
SPLIT FILE  
OFF.
```

\* We produced a line graph with Age/Time/Day on the x-axis and cycles on the y-axis and with a separate line for each of the 2 genomes for gene GFAPvCT.

```
GRAPH  
/LINE(MULTIPLE)MEAN(GFAPvCT) BY Age BY Genotype  
/INTERVAL SE( 1).
```

```
GRAPH  
/LINE(MULTIPLE)MEAN(S100vCT) BY Age BY Genotype  
/INTERVAL SE( 1).
```

```
GRAPH  
/LINE(MULTIPLE)MEAN(VIMENTINvCT) BY Age BY Genotype  
/INTERVAL SE( 1).
```

### 14) Syntax for non parametric test kruskal-wallis test

```
SORT CASES BY Age .  
SPLIT FILE  
SEPARATE BY Age .
```

```
NPAR TESTS  
/K-W=GFAPvCT S100vCT VIMENTINvCT BY Genotype(1 2)  
/MISSING ANALYSIS.
```

### 15) Non-parametric kruskal-wallis test output each gene/age using SPSS

NPar Tests Kruskal-Wallis Test

[DataSet1] H:\research 2007\results stats for thesis as of 5-11-2008\Raw and delta Ct values for glial genes 5-12-2008.sav

Age = PND 7

Ranks<sup>a</sup>

	Genotype	N	Mean Rank
GFAPvCT	Wild type	3	2.00
	Retinal degeneration	3	5.00
	Total	6	
S100vCT	Wild type	3	4.00
	Retinal degeneration	3	3.00
	Total	6	
VIMENTINvCT	Wild type	3	4.00
	Retinal degeneration	3	3.00
	Total	6	

a. Age = PND 7

**Test Statistics<sup>a,b,c</sup>**

	GFAPvCT	S100vCT	VIMENTINvCT
Chi-Square	3.857	.429	.429
df	1	1	1
Asymp. Sig.	.050	.513	.513

- a. Kruskal Wallis Test
- b. Grouping Variable: Genotype
- c. Age = PND 7

**Age = PND 14**

**Ranks<sup>a</sup>**

	Genotype	N	Mean Rank
GFAPvCT	Wild type	3	3.00
	Retinal degeneration	3	4.00
	Total	6	
S100vCT	Wild type	3	2.33
	Retinal degeneration	3	4.67
	Total	6	
VIMENTINvCT	Wild type	3	3.67
	Retinal degeneration	3	3.33
	Total	6	

a. Age = PND 14

**Test Statistics<sup>a,b,c</sup>**

	GFAPvCT	S100vCT	VIMENTINvCT
Chi-Square	.429	2.333	.048
df	1	1	1
Asymp. Sig.	.513	.127	.827

- a. Kruskal Wallis Test
- b. Grouping Variable: Genotype
- c. Age = PND 14

**Age = PND 21**

**Ranks<sup>a</sup>**

	Genotype	N	Mean Rank
GFAPvCT	Wild type	3	2.67
	Retinal degeneration	3	4.33
	Total	6	
S100vCT	Wild type	3	2.67
	Retinal degeneration	3	4.33
	Total	6	
VIMENTINvCT	Wild type	3	2.00
	Retinal degeneration	3	5.00
	Total	6	

a. Age = PND 21

**Test Statistics<sup>a,b,c</sup>**

	GFAPvCT	S100vCT	VIMENTINvCT
Chi-Square	1.190	1.190	3.857
df	1	1	1
Asymp. Sig.	.275	.275	.050

- a. Kruskal Wallis Test
- b. Grouping Variable: Genotype
- c. Age = PND 21

**Age = PND 28**

**Ranks<sup>a</sup>**

	Genotype	N	Mean Rank
GFAPvCT	Wild type	3	4.00
	Retinal degeneration	3	3.00
	Total	6	
S100vCT	Wild type	3	4.67
	Retinal degeneration	3	2.33
	Total	6	
VIMENTINvCT	Wild type	3	3.33
	Retinal degeneration	3	3.67
	Total	6	

a. Age = PND 28

**Test Statistics<sup>a,b,c</sup>**

	GFAPvCT	S100vCT	VIMENTINvCT
Chi-Square	.429	2.333	.048
df	1	1	1
Asymp. Sig.	.513	.127	.827

- a. Kruskal Wallis Test
- b. Grouping Variable: Genotype
- c. Age = PND 28

**Age = PND 35**

**Ranks<sup>a</sup>**

	Genotype	N	Mean Rank
GFAPvCT	Wild type	3	3.33
	Retinal degeneration	3	3.67
	Total	6	
S100vCT	Wild type	3	3.00
	Retinal degeneration	3	4.00
	Total	6	
VIMENTINvCT	Wild type	3	3.00
	Retinal degeneration	3	4.00
	Total	6	

a. Age = PND 35

**Test Statistics<sup>a,b,c</sup>**

	GFAPvCT	S100vCT	VIMENTINvCT
Chi-Square	.048	.429	.429
df	1	1	1
Asymp. Sig.	.827	.513	.513

- a. Kruskal Wallis Test
- b. Grouping Variable: Genotype
- c. Age = PND 35

**Age = PND 42**

**Ranks<sup>a</sup>**

	Genotype	N	Mean Rank
GFAPvCT	Wild type	3	2.67
	Retinal degeneration	3	4.33
	Total	6	
S100vCT	Wild type	3	4.33
	Retinal degeneration	3	2.67
	Total	6	
VIMENTINvCT	Wild type	3	4.67
	Retinal degeneration	3	2.33
	Total	6	

- a. Age = PND 42

**Test Statistics<sup>a,b,c</sup>**

	GFAPvCT	S100vCT	VIMENTINvCT
Chi-Square	1.190	1.190	2.333
df	1	1	1
Asymp. Sig.	.275	.275	.127

- a. Kruskal Wallis Test
- b. Grouping Variable: Genotype
- c. Age = PND 42

**Age = PND 49**

**Ranks<sup>a</sup>**

	Genotype	N	Mean Rank
GFAPvCT	Wild type	3	2.00
	Retinal degeneration	3	5.00
	Total	6	
S100vCT	Wild type	3	2.00
	Retinal degeneration	3	5.00
	Total	6	
VIMENTINvCT	Wild type	3	3.67
	Retinal degeneration	3	3.33
	Total	6	

- a. Age = PND 49

**Test Statistics<sup>a,b,c</sup>**

	GFAPvCT	S100vCT	VIMENTINvCT
Chi-Square	3.857	3.857	.048
df	1	1	1
Asymp. Sig.	.050	.050	.827

- a. Kruskal Wallis Test
- b. Grouping Variable: Genotype
- c. Age = PND 49

**Age = PND 100**

**Ranks<sup>a</sup>**

	Genotype	N	Mean Rank
GFAPvCT	Wild type	3	3.33
	Retinal degeneration	3	3.67
	Total	6	
S100vCT	Wild type	3	3.33
	Retinal degeneration	3	3.67
	Total	6	
VIMENTINvCT	Wild type	3	2.33
	Retinal degeneration	3	4.67
	Total	6	

- a. Age = PND 100

**Test Statistics<sup>a,b,c</sup>**

	GFAPvCT	S100vCT	VIMENTINvCT
Chi-Square	.048	.048	2.333
df	1	1	1
Asymp. Sig.	.827	.827	.127

- a. Kruskal Wallis Test
- b. Grouping Variable: Genotype
- c. Age = PND 100

**Age = PND 140**

**Ranks<sup>a</sup>**

	Genotype	N	Mean Rank
GFAPvCT	Wild type	5	6.00
	Retinal degeneration	5	5.00
	Total	10	
S100vCT	Wild type	5	6.60
	Retinal degeneration	5	4.40
	Total	10	
VIMENTINvCT	Wild type	5	5.40
	Retinal degeneration	5	5.60
	Total	10	

- a. Age = PND 140

**Test Statistics<sup>a,b,c</sup>**

	GFAPvCT	S100vCT	VIMENTINvCT
Chi-Square	.273	1.320	.011
df	1	1	1
Asymp. Sig.	.602	.251	.917

- a. Kruskal Wallis Test
- b. Grouping Variable: Genotype
- c. Age = PND 140

**Age = PND 250**

**Ranks<sup>a</sup>**

	Genotype	N	Mean Rank
GFAPvCT	Wild type	3	2.67
	Retinal degeneration	3	4.33
	Total	6	
S100vCT	Wild type	3	3.33
	Retinal degeneration	3	3.67
	Total	6	
VIMENTINvCT	Wild type	3	3.00
	Retinal degeneration	3	4.00
	Total	6	

- a. Age = PND 250

**Test Statistics<sup>a,b,c</sup>**

	GFAPvCT	S100vCT	VIMENTINvCT
Chi-Square	1.190	.048	.429
df	1	1	1
Asymp. Sig.	.275	.827	.513

- a. Kruskal Wallis Test
- b. Grouping Variable: Genotype
- c. Age = PND 250